Supporting Information

1.Supplementary Figures and Tables

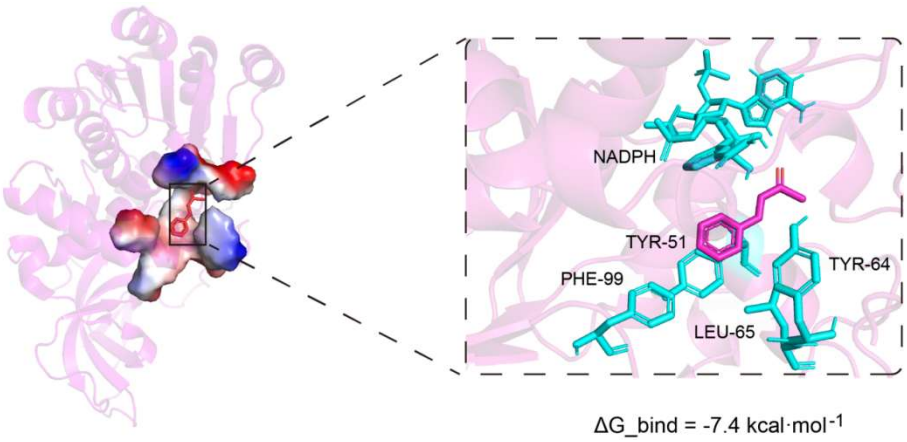

Figure S1. Molecular docking conformations of PTGR2 with NADPH and *trans*-benzylideneacetone with AutoDock Vina. The calculated binding free energy (ΔG_bind) for this conformation is -7.4 kcal·mol^{-1}.

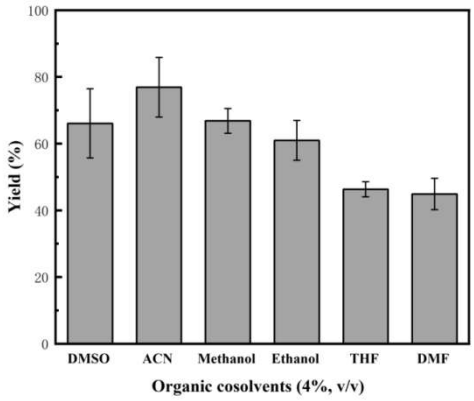

Figure S2. Effect of co-solvent type on the hydrogenation of *trans*-benzylideneacetone using the purified enzyme system.

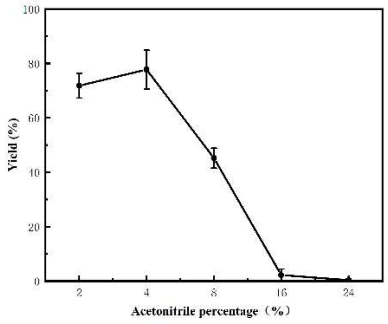

Figure S3. Effect of ACN ratio on the hydrogenation of *trans*-benzylideneacetone using the purified enzyme system.

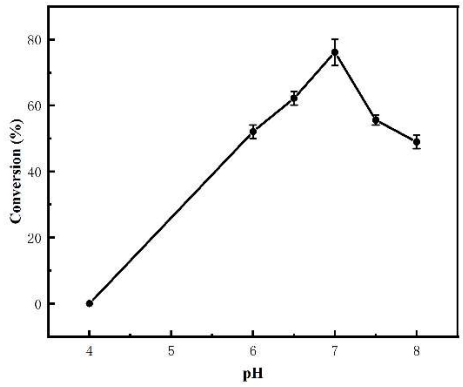

Figure S4. Effect of pH on the hydrogenation of *trans*-benzylideneacetone using the purified enzyme system.

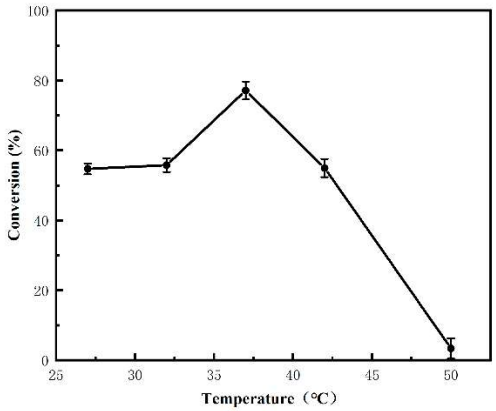

Figure S5. Effects of reaction temperature on the hydrogenation of *trans*-benzylideneacetone using the purified enzyme system.

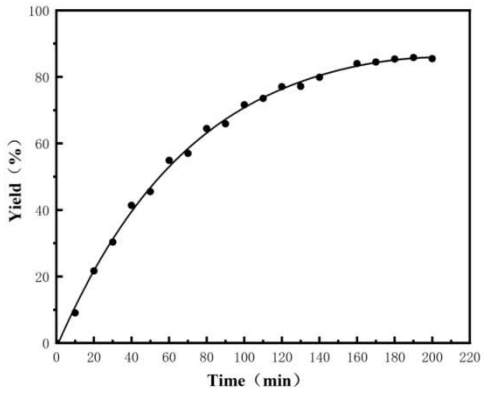

Figure S6. Effects of reaction time on the hydrogenation of *trans*-benzylideneacetone using the purified enzyme system.

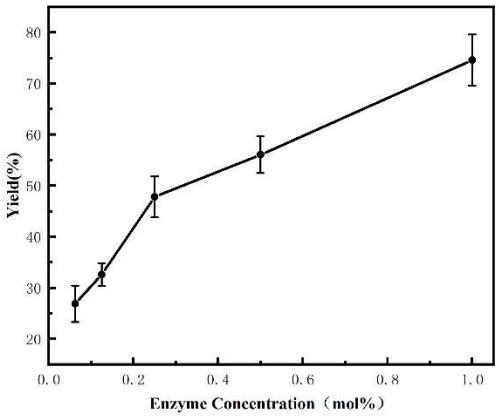

Figure S7. Effects of enzyme concentration on the hydrogenation of *trans*-benzylideneacetone using the purified enzyme system.

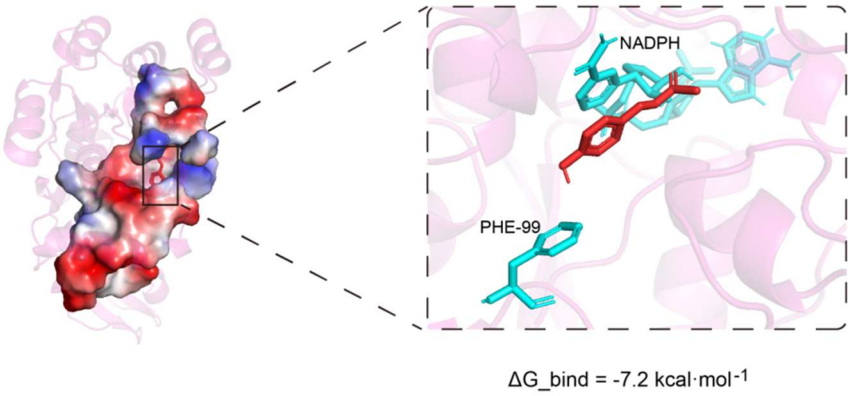

Figure S8. Molecular docking conformations of PTGR2 with NADPH and the precursor to raspberry ketone (1p). The calculated binding free energy (ΔG_bind) for this conformation is -7.2 kcal·mol^{-1}.

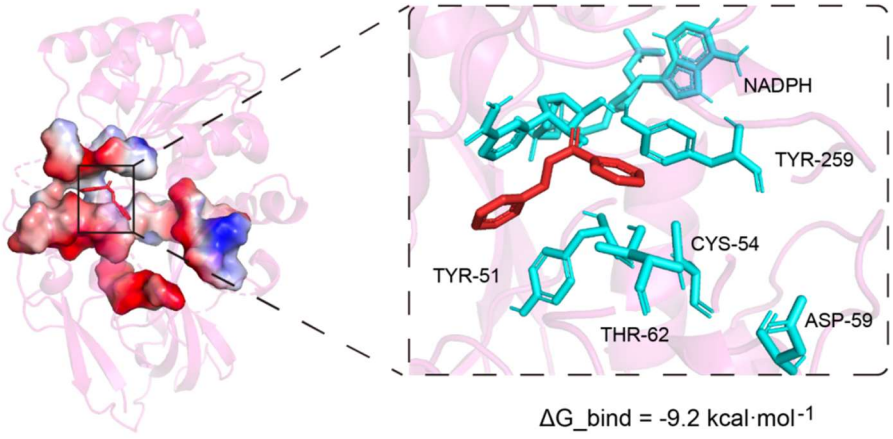

Figure S9. Molecular docking conformations of PTGR2 with NADPH and trans-Chalcone (1q). The calculated binding free energy (ΔG_bind) for this conformation is -9.2 kcal·mol^{-1}.

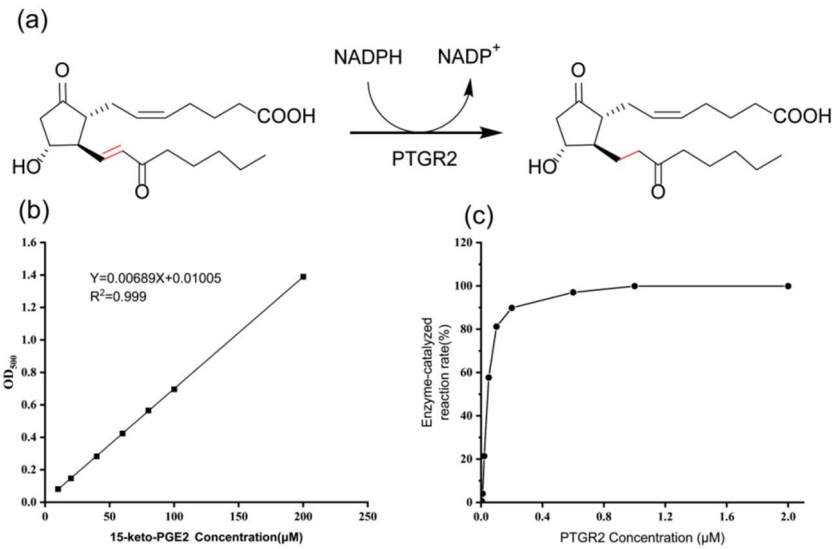

Figure S10. Analysis of PTGR2 catalytic activity. (a) Schematic of the PTGR2-catalyzed reduction of 15-keto-PGE_2. (b) Standard curve correlating 15-keto-PGE_2 concentration with absorbance at 500 nm. (c) Effect of PTGR2 concentration on the enzymatic reaction rate.

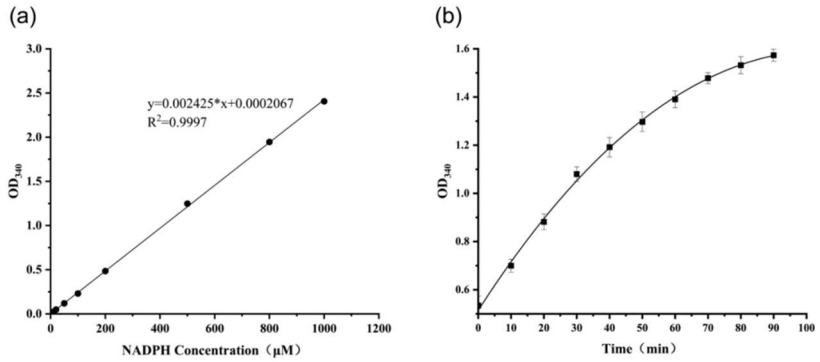

Figure S11. Analysis of GDH catalytic activity. (a) Standard curve of NADPH at 340 nm. (b) Absorbance of the reaction system at 340 nm measured at different time points.

Table S1. Gradient elution procedure of preparative HPLC Purification

Time/min	Solution A/%	Solution B/%
0	95	5
10	95	5
40	5	95
50	5	95

2.General Information

All commercial reagents and solvents were purchased from Bide Pharmatech, Macklin, and Adamas with the highest purity available and used as received. The protein expression strain, plasmid, and competent *E. coli* cells were purchased from Sangon Biotech (Shanghai) Co., Ltd.

NMR spectra were recorded on a Bruker AVANCE NEO 400 spectrometer at 400 MHz(1H). Chemical shifts (δ) are reported in parts per million (ppm) relative to Me4Si (δ 0.00) using deuterated solvent (DMSO-d_6, CD_3OD or $CDCl_3$) as an internal standard. The NMR signals are described as singlet (*s*), doublet (*d*), or multiplet (*m*), and the coupling constants are given in hertz (Hz).

Column chromatography was performed using silica gel (300–400 mesh). Reaction progress was monitored by thin-layer chromatography (TLC) visualized under UV light (254 nm or 365 nm). Preparative high-performance liquid chromatography (HPLC) was carried out on an Agilent 1260 Infinity II system. Gas chromatography–mass spectrometry (GC–MS) analyses were performed using an Agilent 8890 GC system coupled with an Agilent 5977C MSD. Absorbance measurements were recorded using an Agilent BioTek Epoch 2 microplate reader.

3.Protein and DNA Sequences

3.1 C-His-PTGR2 (*Mus musculus*) sequence

Protein sequence

MIIQRVVLNSRPGKNGNPVAENFRVEEFSLPDALNEGQVQVRTLYLSVDPYMRCKM
NEDTGTDYLAPWQLAQVADGGGIGVVEESKHQKLTKGDFVTSFYWPWQTKAILDG
NGLEKVDPQLVDGHLSYFLGAIGMPGLTSLIGVQEKGHISAGSNQTMVVSGAAGAC
GSLAGQIGHLLGCSRVVGICGTQEKCLFLTSELGFDAAVNYKTGNVAEQLREACPG
GVDVYFDNVGGDISNAVISQMNENSHIILCGQISQYSNDVPYPPPLPPAVEAIRKER
NITRERFTVLNYKDKFEPGILQLSQWFKEGKLKVKETMAKGLENMGVAFQSMMTG
GNVGKQIVCISEDSSLHHHHHH

DNA sequence

ATGATCATACAAAGAGTGGTATTGAATTCCCGACCTGGGAAAAATGGAAATCCA
GTCGCAGAGAACTTCAGGGTGGAAGAGTTCAGTTTACCGGATGCTCTCAATGAA
GGTCAAGTTCAAGTGAGGACTCTTTATCTCTCGGTGGATCCTTACATGCGCTGT
AAGATGAACGAGGACACTGGCACTGACTACTTGGCACCGTGGCAGCTGGCGCA
GGTGGCTGATGGTGGAGGAATTGGAGTTGTAGAGGAGAGCAAGCACCAGAAGT
TGACTAAAGGCGATTTTGTGACTTCGTTTTACTGGCCCTGGCAAACTAAGGCAA

TTCTAGATGGGAATGGCCTTGAAAAGGTAGACCCACAACTTGTAGATGGACACC
TTTCATATTTTCTTGGGGCTATAGGTATGCCTGGCTTGACTTCCTTGATTGGGGT
ACAGGAGAAAGGCCATATATCTGCTGGATCTAATCAGACAATGGTTGTCAGTGG
AGCAGCAGGCGCCTGTGGATCTTTGGCTGGGCAGATTGGCCACCTGCTTGGCT
GTTCCAGAGTGGTGGGAATTTGTGGAACGCAGGAGAAATGTCTCTTTTTGACCT
CAGAGCTGGGGTTTGATGCTGCAGTTAATTACAAAACAGGGAATGTGGCAGAG
CAGCTGCGAGAAGCGTGCCCGGGCGGAGTGGATGTCTACTTTGACAATGTTGG
AGGTGACATCAGCAACGCGGTGATAAGTCAGATGAATGAGAACAGCCACATCAT
CCTGTGTGGTCAGATTTCTCAGTACAGTAACGATGTGCCCTACCCTCCTCCACT
GCCCCCTGCAGTAGAAGCCATCCGGAAGGAACGAAACATCACAAGAGAGAGAT
TTACGGTATTAAATTATAAAGATAAATTTGAGCCTGGAATTCTACAGCTGAGTCA
GTGGTTTAAAGAAGGAAAGCTAAAGGTCAAGGAGACCATGGCAAAGGGCTTGG
AAAACATGGGAGTTGCATTCCAGTCCATGATGACAGGGGGCAACGTAGGGAAA
CAGATCGTCTGCATTTCAGAAGATTCTTCTCTGCACCACCACCACCACCACTAG

3.2 C-His-GDH (*Priestia megaterium*) sequence

Protein sequence

MYTDLKDKVVVITGGSTGLGRAMAVRFGQEEAKVVINYYNNEEEALDAKKEVEEAG

GQAIIVQGDVTKEEDVVNLVQTAIKEFGTLDVMINNAGVENPVPSHELSLDNWNKVI

DTNLTGAFLGSREAIKYFVENDIKGNVINMSSVHEMIPWPLFVHYAASKGGMKLMTE

TLALEYAPKGIRVNNIGPGAMNTPINAEKFADPVQRADVESMIPMGYIGKPEEVAAV

AAFLASSQASYVTGITLFADGGMTKYPSFQAGRGHHHHHH

DNA sequence

ATGTATACAGATTTAAAAGATAAAGTAGTTGTAATTACAGGTGGATCAACAGGTT

TAGGACGTGCAATGGCTGTTCGTTTCGGTCAAGAAGAAGCAAAAGTTGTTATTA

ACTATTACAACAATGAAGAAGAAGCTTTAGATGCGAAAAAAGAAGTAGAAGAAG

CAGGCGGACAAGCAATCATCGTTCAAGGCGACGTAACAAAAGAAGAAGACGTT

GTAAACCTTGTTCAAACAGCTATTAAAGAATTCGGAACATTAGACGTTATGATTA

ATAACGCTGGTGTTGAAAACCCAGTTCCTTCTCATGAGCTATCTTTAGACAACTG

GAACAAAGTTATTGATACAAACTTAACAGGTGCATTCTTAGGAAGCCGTGAAGC

AATTAAATATTTCGTTGAAAATGACATTAAAGGAAACGTTATTAACATGTCCAGC

GTTCACGAAATGATTCCTTGGCCATTATTTGTTCACTACGCAGCAAGTAAAGGC

GGTATGAAACTAATGACGGAAACATTGGCTCTTGAATATGCGCCAAAAGGTATC

CGAGTAAATAACATTGGACCAGGTGCGATGAACACACCAATTAACGCTGAAAAA

TTCGCTGATCCTGTACAACGTGCAGACGTAGAAAGCATGATTCCAATGGGTTAC
ATCGGTAAGCCAGAAGAAGTAGCAGCAGTTGCAGCATTCTTAGCATCATCACAA
GCAAGCTATGTAACAGGTATTACATTATTTGCTGATGGTGGTATGACGAAATACC
CTTCTTTCCAAGCAGGAAGAGGCCACCACCACCACCACCACTAA

4.Protein Structure Modeling and Molecular Docking

Ligand Preparation. The two-dimensional (2D) structure of the substrate was sketched using ChemDraw (Ver 19.0) and saved in SDF format. The structure was then subjected to energy minimization using Chem3D and subsequently converted to the PDB format. The ligand was prepared by adding hydrogen atoms and defining rotatable bonds.

Protein Preparation. The crystal structure of the PTGR2 (PDB ID: 2ZB3) at a resolution of 2.00 Å was downloaded from the RCSB Protein Data Bank. The protein was prepared for docking by removing all water molecules, adding polar hydrogen atoms, and computing Gasteiger charges. The prepared receptor was saved in the PDBQT format.

Molecular Docking. Semi-flexible docking was performed using AutoDock Vina, treating the receptor as rigid and the ligand as flexible. The resulting binding poses were visualized with PyMOL (Ver 2.5.4), and the binding affinity was evaluated based on the docking score ($kcal \cdot mol^{-1}$).[1, 2]

5.Experimental Details

5.1 Cloning, Expression and Purification of Enzymes

5.1.1 Cloning and Expression of PTGR2

The recombinant plasmid pET-28a(+)-PTGR2 was transformed into *E. coli* BL21(DE3) competent cells. The expression strain was selected on Luria-Bertani (LB) agar plates containing 50 μg/mL kanamycin. This strain was inoculated into 5 mL of liquid LB medium containing the aforementioned antibiotic and cultured overnight at 37 °C with shaking at 200 rpm. Subsequently, the overnight culture was inoculated into 1 L of the

same medium and grown until the OD_{600} reached ~0.6. Isopropyl β-D-1-thiogalactopyranoside (IPTG) was added to a final concentration of 0.25 mM, and protein expression was induced for 16 hours at 16 °C. Following induction, the cells were harvested by centrifugation (4500 rpm, 4 °C, 10 min). The cell pellets were stored at -20 °C until further use.

5.1.2 Cloning and expression of GDH

The recombinant plasmid pET-21a(+)-GDH was transformed into *E. coli* BL21(DE3) competent cells. The expression strain was selected on LB agar plates containing 100 μg/mL ampicillin. This strain was inoculated into 5 mL of liquid LB medium containing the aforementioned antibiotic and cultured overnight at 37 °C with shaking at 200 rpm. Subsequently, the overnight culture was inoculated into 1 L of the same medium and grown until the OD_{600} reached ~0.6. IPTG was added to a final concentration of 0.20 mM, and protein expression was induced for 16 hours at 16 °C. Following induction, the cells were harvested by centrifugation (4500 rpm, 4 °C, 10 min). The cell pellets were stored at -20 °C until further use.

5.1.3 Preparation and Purification of PTGR2 and GDH

The harvested bacterial pellets were resuspended in 10 mL of lysis buffer (20 mM Tris, 150 mM NaCl, 0.2% Triton X-100, pH 8.0) and disrupted by sonication in an ice-water bath (200 W power; 2 s on, 4 s off pulses; 15 min total sonication time). The cell lysate was clarified by centrifugation at 12,000 rpm for 30 min at 4 °C, and the supernatant was collected and filtered through a 0.45 μm membrane. The protein was purified by immobilized metal affinity chromatography (IMAC) on a Bio-Rad NGC system. The filtered supernatant was loaded onto a Ni-NTA Profinity™ IMAC column pre-equilibrated with equilibrium buffer (20 mM Tris, 150 mM NaCl, pH 8.0). After washing, the bound protein was eluted with a step gradient of imidazole (5, 20, 40, 100, and 500 mM). The desired fractions were identified by SDS-PAGE, then pooled, concentrated, and buffer-exchanged into 100 mM Tris·HCl (pH 7.0) using a 10 kDa MWCO

ultrafiltration device. The final protein concentration was determined using a BioTek Synergy H1 microplate reader. The purified protein was aliquoted and stored at -20 °C.

5.2 *In Vitro* Enzyme Activity Assay

5.2.1 *In Vitro* Enzyme Activity Assay of PTGR2

The in vitro activity of PTGR2 (an NADPH-dependent prostaglandin reductase) was determined colorimetrically by monitoring the consumption of its substrate, 15-keto-PGE_2 (Figure S10a). This assay relies on the formation of a red-colored species by the substrate under alkaline conditions.[3] First, a standard curve of 15-keto-PGE_2 was established, which demonstrated excellent linearity (R^2=0.999, Figure S10b). Subsequently, the effect of enzyme concentration was investigated at a fixed initial substrate concentration of 60 μM. The results showed that the reaction rate reached saturation at a PTGR2 concentration of 1 μM or higher (Figure S10c).

5.2.2 *In Vitro* Enzyme Activity Assay of GDH

The enzymatic activity of purified glucose dehydrogenase (GDH) was determined spectrophotometrically by monitoring the increase in absorbance at 340 nm, corresponding to the reduction of $NADP^+$ to NADPH. The assay was performed in a 96-well microplate with a total volume of 200 μL. The reaction mixture contained 100 mM Tris-HCl (pH 7.0), 20 mM glucose, 0.5 mM $NADP^+$, and 4 μM purified GDH. Reactions were incubated at 37 °C, and absorbance was continuously monitored using a microplate reader. Quantification based on an NADPH standard curve indicated that 4 μM GDH catalyzed the formation of 76 μM NADPH over a 10-minute period (Figure S11). These results confirm the catalytic activity of the purified GDH and demonstrate its suitability for *in vitro* cofactor regeneration.

5.3 Construction of the PTGR2-GDH Co-expression Strain

The recombinant plasmids pET-28a(+)-PTGR2 and pET-21a(+)-GDH were co-transformed into *E. coli* BL21(DE3) competent cells. The co-expression strain, *E. coli* (PTGR2/GDH), was selected on LB agar plates containing 100 μg/mL Amp and 50 μg/mL Kana. This strain was inoculated into 5 mL of liquid LB medium containing the aforementioned dual antibiotics and cultured overnight at 37 °C with shaking at 200 rpm. Subsequently, the overnight culture was inoculated into 1 L of the same medium and grown until the OD_{600} reached ~0.6. IPTG was added to a final concentration of 0.25 mM, and protein co-expression was induced for 16h at 16 °C. Following induction, the cells were harvested by centrifugation (4500 rpm, 4 °C, 10 min) and resuspended in 20 mL of lysis buffer. The cell suspension was disrupted by sonication in an ice-water bath, and the supernatant was collected after high-speed centrifugation (12,000 rpm, 4 °C, 30 min). Finally, the successful co-expression of PTGR2 and GDH proteins was verified by affinity chromatography and SDS-PAGE.

5.4 Biocatalytic Reactions

5.4.1 Optimization of Reaction Conditions for the PTGR2-GDH System

The reaction conditions for the PTGR2-GDH-catalyzed reduction of *trans*-benzylideneacetone were optimized in a 100 mM Tris-HCl buffer system using a one-variable-at-a-time approach. The influence of several key parameters on enzymatic activity was investigated, including the type and concentration of cosolvent, pH, temperature, substrate concentration, and reaction time(Figures S4-S9). The final optimized conditions were determined to be: 4% (v/v) acetonitrile (ACN) as the cosolvent, pH 7.0, 37 °C, 1 mol% PTGR2, and a reaction time of 3 hours. The reaction yield was quantified by GC-MS analysis.

5.4.2 General Procedure for Purified PTGR2-GDH Enzyme Catalysis

The coupled-enzyme reaction was performed in a total volume of 1mL in 100 mM Tris-

HCl buffer (pH 7.0). The system contained the substrate (1 μmol), $NADP^+$ (1 eq.), glucose (200 eq.), 4% (v/v) ACN, PTGR2 (1 mol%), and GDH (2 mol%). The reaction was carried out at 37 °C with shaking at 800 rpm for 3 h. The reaction was subsequently quenched with ethyl acetate and extracted three times. The combined organic phases were dried over anhydrous Na_2SO_4, filtered, and the solvent was removed under reduced pressure. The reaction yield was quantified by GC-MS analysis.

5.4.3 General Procedure for Whole-Cell Biotransformation

The whole-cell biotransformation was performed in a 10 mL total volume using a 100 mM Tris-HCl buffer (pH 7.0). The reaction system was composed of the substrate (10 μmol), $NADP^+$ (1 eq.), glucose (200 eq.), 4% (v/v) ACN, and *E. coli* cells co-expressing PTGR2 and GDH (OD_{600} = 1.54). The mixture was incubated at 37 °C for 12 h with shaking at 200 rpm. Subsequently, the reaction was terminated by the addition of ethyl acetate. The mixture was extracted three times with ethyl acetate. The combined organic layers were dried over anhydrous Na_2SO_4, filtered, and concentrated under reduced pressure. The reaction yield was quantified by GC-MS analysis.

Preparative-scale biotransformation of substrates **1a**, **1i**, and **1r** (150 μmol each) was performed in 150 mL of 100 mM Tris-HCl buffer (pH 7.0) under the same conditions described above. The resulting products, **2a**, **2i**, and **2r**, were purified by preparative HPLC to determine their isolated yields.

5.4.4 Competitive Inhibition of PTGR2 Activity by Natural Compounds

To investigate the competitive inhibitory effects of various natural compounds on PTGR2 activity, 50 μM 15-keto-PGE_2 and 2 μM PTGR2 were pre-incubated at 37 °C for 10 min. The standard reaction buffer used for this assay consisted of 100 mM Tris-HCl (pH 7.0), 1.0 mM EDTA and 1.0 mM DTT. Following the pre-incubation period, different concentrations of the compounds (0–10 mM) with 300 μM NADPH were

added to the enzyme-inhibitor mixture to initiate the reaction, which was then performed at 37 °C for 15 minutes. The reaction was terminated by the subsequent addition of 20 μL of 2 N NaOH solution. The concentration of the remaining 15-keto-PGE_2 was quantified by measuring the maximum absorption at 500 nm. Blank controls included both the no-enzyme group and the no-competitive-inhibitor group. The experimental results are expressed as the mean percentages ± standard error (SE) of inhibition relative to the control values, based on three determinations.[3]

5.4.5 Analysis and Purification Methods

GC-MS analysis was performed using a gas chromatograph coupled with a mass selective detector (MSD) and equipped with an HP-5 column (Agilent, 25 m × 0.25 mm × 0.25 μm). The injector temperature was set to 320 °C, with a split ratio of 25:1 and a linear velocity of 40 cm/s. The oven temperature program was as follows: initial hold at 100 °C for 2 min, increased to 310 °C at a rate of 15 °C/min, and held for 3 min.

Purification of the target compounds was achieved by preparative HPLC using a CSTCHROM (Daiso C18, 10 μm, 20 × 250 mm) column. The mobile phase comprised ultrapure water (A) and acetonitrile (B). The separation was carried out at a column temperature of 35 °C with a flow rate of 4.0 mL/min, and the eluent was monitored at 210 nm. For each run, an injection volume of 2.0 mL was used. The elution program is described in Table S1.

6. General Procedures of Chemical Synthesis

6.1 General Procedure 1

To a solution of the benzaldehyde derivative (10 mmol) in a mixture of acetone and water (6 mL, v/v = 1:1), 3 mL of a 1% aqueous sodium hydroxide solution was added dropwise. The resulting mixture was stirred at 65 °C for 12 hours.[4] After completion,

the mixture was extracted with CH_2Cl_2 (3 × 15 mL). The combined organic layers were concentrated in vacuo, and the crude product was purified by column chromatography.

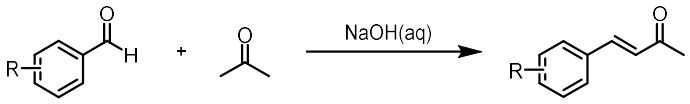

6.2 General Procedure 2

To a round-bottom flask were sequentially added 3-pentanone or 4-heptanone (50 mmol), benzaldehyde (50 mmol), and concentrated hydrochloric acid (15 mL). The mixture was heated to reflux for 4 hours. After completion, the mixture was extracted with CH_2Cl_2 (3 × 15 mL).[5] The combined organic layers were concentrated in vacuo, and the crude product was purified by column chromatography.

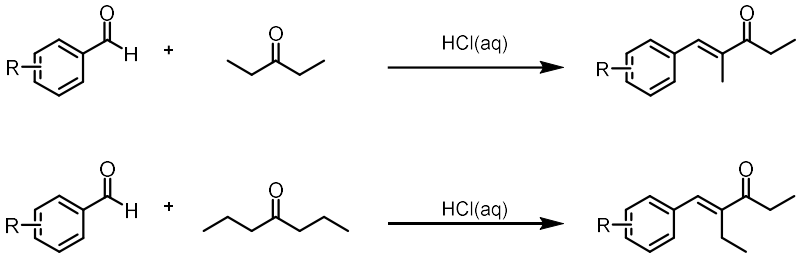

6.3 General Procedure 3

A mixture of the unsaturated enone (10 mmol) and 10% Pd/C (1.0 mmol) in methanol (15 mL) was placed in a round-bottom flask. The vessel was evacuated and backfilled with H_2 (3 cycles), and the reaction was stirred under a hydrogen atmosphere (1 atm, balloon) at ambient temperature for 12 h.[6] The catalyst was subsequently removed by filtration through Celite®. After evaporation of the solvent in vacuo, the residue was purified by preparative HPLC.

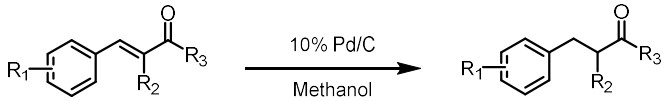

7. Analytical data of all synthesis products

(*E*)-4-(3-fluorophenyl)but-3-en-2-one (1b)

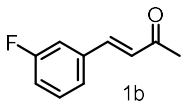

Compound **1b** was synthesized following **General Procedure 1**.

A yellow solid, 46% yield.

^{1}H NMR (400 MHz, CDCl3) δ 7.47 (d, *J* = 16.3 Hz, 1H), 7.39 – 7.30 (m, 2H), 7.24 (d, *J* = 9.8 Hz, 1H), 7.13 – 7.07 (m, 1H), 6.71 (d, *J* = 16.3 Hz, 1H), 2.39 (s, 3H).

The spectral data match those reported.[7]

(*E*)-4-(4-fluorophenyl)but-3-en-2-one (1c)

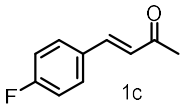

Compound **1c** was synthesized following **General Procedure 1**.

A white solid, 63% yield.

^{1}H NMR (400 MHz, CDCl3) δ 7.59 – 7.42 (m, 3H), 7.09 (t, *J* = 8.5 Hz, 2H), 6.64 (d, *J* = 16.3 Hz, 1H), 2.37 (s, 3H).

The spectral data match those reported.[7]

(*E*)-4-(2-chlorophenyl)but-3-en-2-one (1d)

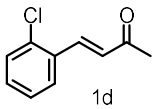

Compound **1d** was synthesized following **General Procedure 1**.

A white solid, 58% yield.

^{1}H NMR (400 MHz, CDCl3) δ 7.95 (d, *J* = 16.4 Hz, 1H), 7.66 (d, *J* = 7.3 Hz, 1H), 7.45 (d, *J* = 8.0 Hz, 1H), 7.37 – 7.28 (m, 2H), 6.68 (d, *J* = 16.8 Hz, 1H), 2.44 (s, 3H).

The spectral data match those reported.[8]

(*E*)-4-(2-bromophenyl)but-3-en-2-one (1f)

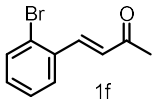

1f

Compound **1f** was synthesized following **General Procedure 1**.

A light yellow liquid, 55% yield.

^{1}H NMR (400 MHz, CDCl3) δ 7.91 (d, *J* = 16.3 Hz, 1H), 7.64 (d, *J* = 8.0 Hz, 2H), 7.36 (t, *J* = 7.6 Hz, 1H), 7.29 – 7.24 (m, 1H), 6.64 (d, *J* = 16.3 Hz, 1H), 2.44 (s, 3H).

The spectral data match those reported.[8]

(*E*)-3-(3-oxobut-1-en-1-yl)benzonitrile (1h)

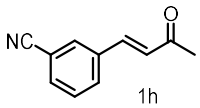

1h

Compound **1h** was synthesized following **General Procedure 1**.

A white solid, 70% yield.

^{1}H NMR (400 MHz, CDCl3) δ 7.82 – 7.74 (m, 2H), 7.67 (d, *J* = 6.5 Hz, 1H), 7.55 – 7.43 (m, 2H), 6.75 (d, *J* = 16.3 Hz, 1H), 2.40 (s, 3H).

The spectral data match those reported.[9]

(*E*)-4-(3-oxobut-1-en-1-yl)benzonitrile (1i)

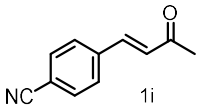

1i

Compound **1i** was synthesized following **General Procedure 1**.

A light yellow liquid, 65% yield.

^{1}H NMR (400 MHz, CD3OD) δ 7.85 – 7.73 (m, 4H), 7.65 (d, *J* = 16.4 Hz, 1H), 6.90 (d, *J* = 16.4 Hz, 1H), 2.40 (s, 3H).

The spectral data match those reported.[10]

(*E*)-4-(*m*-tolyl)but-3-en-2-one (1j)

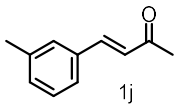

Compound **1j** was synthesized following **General Procedure 1**.

A yellow liquid, 62% yield .

^{1}H NMR (400 MHz, CDCl3) δ 7.51 (d, *J* = 16.3 Hz, 1H), 7.41 – 7.18 (m, 4H), 6.73 (d, *J* = 16.3 Hz, 1H), 2.40 (s, 6H).

The spectral data match those reported.[8]

(*E*)-4-(*p*-tolyl)but-3-en-2-one (1k)

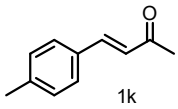

Compound **1k** was synthesized following **General Procedure 1**.

A yellow solid, 42% yield.

^{1}H NMR (400 MHz, CDCl3) δ 7.52 – 7.41 (m, 3H), 7.20 (d, *J* = 7.9 Hz, 2H), 6.68 (d, *J* = 16.3 Hz, 1H), 2.38 (s, 3H), 2.37 (s, 3H).

The spectral data match those reported.[7]

(*E*)-2-methyl-1-(*p*-tolyl)pent-1-en-3-one (1l)

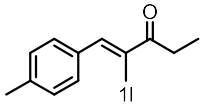

Compound **1l** was synthesized following **General Procedure 2**.

A light yellow liquid, 45% yield.

^{1}H NMR (400 MHz, CDCl3) δ 7.38 (s, 1H), 7.22 (d, *J* = 7.8 Hz, 2H), 7.09 (d, *J* = 7.9 Hz, 2H), 2.68 (qd, *J* = 7.2, 1.3 Hz, 2H), 2.26 (s, 3H), 1.98 (s, 3H), 1.07 (td, *J* = 7.2, 1.4 Hz, 3H).

The spectral data match those reported.[11]

(*E*)-4-(4-methoxyphenyl)but-3-en-2-one (1m)

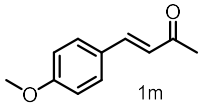

Compound **1m** was synthesized following **General Procedure 1**.

A pale yellow solid, 72% yield.

^{1}H NMR (400 MHz, CD3OD) δ 7.64 – 7.57 (m, 3H), 6.97 (d, *J* = 8.8 Hz, 2H), 6.66 (d, *J* = 16.3 Hz, 1H), 3.84 (s, 3H), 2.36 (s, 3H).

The spectral data match those reported.[7]

(*E*)-1-(4-methoxyphenyl)-2-methylpent-1-en-3-one (1n)

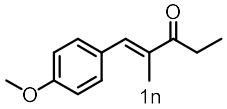

Compound **1n** was synthesized following **General Procedure 2**.

A light yellow liquid, 33% yield.

^{1}H NMR (400 MHz, CDCl3) δ 7.48 (s, 1H), 7.40 (d, *J* = 8.7 Hz, 2H), 6.94 (d, *J* = 8.8 Hz, 2H), 3.84 (s, 3H), 2.83 (q, *J* = 7.3 Hz, 2H), 2.08 (d, *J* = 1.1 Hz, 3H), 1.17 (t, *J* = 7.3 Hz, 3H).

The spectral data match those reported.[11]

(*E*)-3-(4-methoxybenzylidene)heptan-4-one (1o)

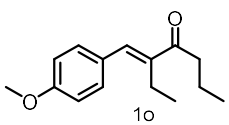

Compound **1o** was synthesized following **General Procedure 2.**

A pale yellow liquid, 50% yield.

^{1}H NMR (400 MHz, CDCl3) δ 7.40 (d, *J* = 4.1 Hz, 2H), 7.37 (d, *J* = 2.1 Hz, 1H), 6.98 – 6.91 (m, 2H), 3.85 (s, 3H), 2.75 (t, *J* = 7.4 Hz, 2H), 2.56 (q, *J* = 7.5 Hz, 2H), 1.70 (h, *J* = 7.2 Hz, 2H), 1.10 (t, *J* = 7.4 Hz, 3H), 0.98 (t, *J* = 7.4 Hz, 3H).

The spectral data match those reported.[12]

4-phenylbutan-2-one (2a)

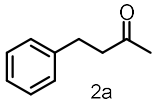

Compound **2a** was synthesized following **General Procedure 3.**

A pale yellow liquid, 90% yield.

^{1}H NMR (400 MHz, CDCl3) δ 7.33 – 7.28 (m, 2H), 7.22 (t, *J* = 7.0 Hz, 3H), 2.92 (t, *J* = 7.6 Hz, 2H), 2.79 (t, *J* = 7.5 Hz, 2H), 2.17 (s, 3H).

The spectral data match those reported.[13]

4-(3-fluorophenyl)butan-2-one (2b)

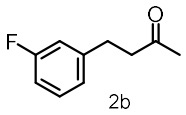

Compound **2b** was synthesized following **General Procedure 3.**

A pale yellow liquid, 63% yield.

^{1}H NMR (400 MHz, CDCl3) δ 7.29 – 7.23 (m, 1H), 6.98 (d, *J* = 7.8 Hz, 1H), 6.93 – 6.88 (m, 2H), 2.91 (t, *J* = 7.5 Hz, 2H), 2.78 (t, *J* = 7.5 Hz, 2H), 2.17 (s, 3H).

The spectral data match those reported.[14]

4-(4-fluorophenyl)butan-2-one (2c)

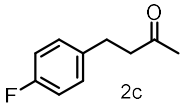

Compound **2c** was synthesized following **General Procedure 3.**

A pale yellow liquid, 59% yield.

^{1}H NMR (400 MHz, CDCl3) δ 7.15 – 7.11 (m, 2H), 6.98 – 6.93 (m, 2H), 2.86 (t, *J* = 7.4 Hz, 2H), 2.73 (t, *J* = 7.4 Hz, 2H), 2.13 (s, 3H).

The spectral data match those reported.[13]

4-(2-chlorophenyl)butan-2-one (2d)

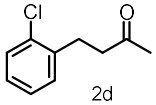

2d

Compound **2d** was synthesized following **General Procedure 3.**

A pale yellow liquid, 49% yield.

^{1}H NMR (400 MHz, CDCl3) δ 7.36 (d, *J* = 7.3 Hz, 1H), 7.29 – 7.24 (m, 1H), 7.19 (tt, *J* = 7.0, 3.8 Hz, 2H), 3.02 (t, *J* = 7.6 Hz, 2H), 2.79 (t, *J* = 7.6 Hz, 2H), 2.18 (s, 3H).

The spectral data match those reported.[14]

4-(4-chlorophenyl)butan-2-one (2e)

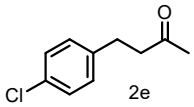

2e

Compound **2e** was synthesized following **General Procedure 3.**

A pale yellow liquid, 53% yield.

^{1}H NMR (400 MHz, CDCl3) δ 7.27 (d, *J* = 5.3 Hz, 1H), 7.25 (d, *J* = 1.9 Hz, 1H), 7.13 (d, *J* = 8.4 Hz, 2H), 2.88 (t, *J* = 7.4 Hz, 2H), 2.75 (t, *J* = 7.4 Hz, 2H), 2.15 (s, 3H).

The spectral data match those reported.[14]

4-(2-bromophenyl)butan-2-one (2f)

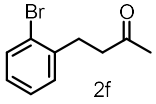

2f

Compound **2f** was synthesized following **General Procedure 3.**

A pale yellow liquid, 56% yield.

^{1}H NMR (400 MHz, DMSO-d_6) δ 7.63 – 7.53 (m, 1H), 7.37 – 7.27 (m, 2H), 7.15 (ddd, *J* = 8.0, 6.6, 2.5 Hz, 1H), 2.89 – 2.84 (m, 2H), 2.80 – 2.74 (m, 2H), 2.12 (s, 3H).

The spectral data match those reported.[14]

4-(4-bromophenyl)butan-2-one (2g)

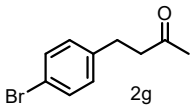

2g

Compound **2g** was synthesized following **General Procedure 3.**

A pale yellow liquid, 69% yield.

^{1}H NMR (400 MHz, CDCl3) δ 7.39 (d, *J* = 8.2 Hz, 2H), 7.05 (d, *J* = 8.2 Hz, 2H), 2.84 (t, *J* = 7.4 Hz, 2H), 2.73 (t, *J* = 7.3 Hz, 2H), 2.13 (s, 3H).

The spectral data match those reported.[14]

3-(3-oxobutyl)benzonitrile (2h)

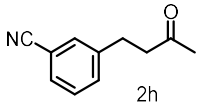

2h

Compound **2h** was synthesized following **General Procedure 3.**

A pale yellow liquid, 74% yield.

^{1}H NMR (400 MHz, CDCl3) δ 7.52 – 7.48 (m, 2H), 7.45 (d, *J* = 7.8 Hz, 1H), 7.39 (t, *J* = 7.9 Hz, 1H), 2.94 (t, *J* = 7.3 Hz, 2H), 2.80 (t, *J* = 7.3 Hz, 2H), 2.17 (s, 3H).

The spectral data match those reported.[15]

4-(4-isocyanophenyl)butan-2-one (2i)

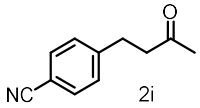

2i

Compound **2i** was synthesized following **General Procedure 3.**

A pale yellow liquid, 79% yield.

^{1}H NMR (400 MHz, CDCl3) δ 7.54 (d, *J* = 8.1 Hz, 2H), 7.28 (d, *J* = 8.1 Hz, 2H), 2.93 (t, *J* = 7.4 Hz, 2H), 2.77 (t, *J* = 7.4 Hz, 2H), 2.13 (s, 3H).

The spectral data match those reported.[15]

4-(*m*-tolyl)butan-2-one (2j)

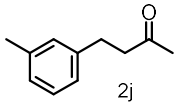

Compound **2j** was synthesized following **General Procedure 3.**

A pale yellow liquid, 88% yield.

^{1}H NMR (400 MHz, CDCl3) δ 7.17 (t, *J* = 7.6 Hz, 1H), 7.00 (t, *J* = 9.2 Hz, 3H), 2.85 (d, *J* = 7.5 Hz, 2H), 2.78 – 2.72 (m, 2H), 2.33 (s, 3H), 2.14 (s, 3H).

The spectral data match those reported.[13]

4-(*p*-tolyl)butan-2-one (2k)

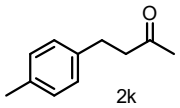

Compound **2k** was synthesized following **General Procedure 3.**

A pale yellow liquid, 87% yield.

^{1}H NMR (400 MHz, CDCl3) δ 7.09 (d, *J* = 4.9 Hz, 2H), 7.08 (s, 2H), 2.88 – 2.83 (m, 2H), 2.76 – 2.71 (m, 2H), 2.31 (s, 3H), 2.14 (s, 3H).

The spectral data match those reported.[14]

2-methyl-1-(*p*-tolyl)pentan-3-one (2l)

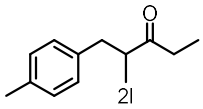

Compound **2l** was synthesized following **General Procedure 3.**

A pale yellow liquid, 78% yield.

^{1}H NMR (400 MHz, CDCl3) δ 7.08 (d, *J* = 7.9 Hz, 2H), 7.03 (d, *J* = 8.1 Hz, 2H), 2.94 (dd, *J* = 13.3, 7.2 Hz, 1H), 2.82 (h, *J* = 7.0 Hz, 1H), 2.58 – 2.36 (m, 2H), 2.31 (s, 3H), 2.26 (dt, *J* = 17.8, 7.2 Hz, 1H), 1.08 (d, *J* = 6.9 Hz, 3H), 0.99 (t, *J* = 7.3 Hz, 3H).

The spectral data match those reported.[16]

4-(4-methoxyphenyl)butan-2-one (2m)

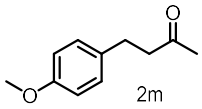

Compound **2m** was synthesized following **General Procedure 3.**

A pale yellow liquid, 82% yield.

^{1}H NMR (400 MHz, CDCl3) δ 7.10 (d, *J* = 8.6 Hz, 2H), 6.86 – 6.77 (m, 2H), 3.78 (s, 3H), 2.88 – 2.79 (m, 2H), 2.76 – 2.67 (m, 2H), 2.13 (s, 3H).

The spectral data match those reported.[13]

1-(4-methoxyphenyl)-2-methylpentan-3-one (2n)

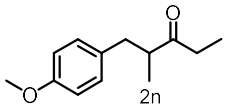

Compound **2n** was synthesized following **General Procedure 3.**

A pale yellow liquid, 57% yield.

^{1}H NMR (400 MHz, CDCl3) δ 7.05 (d, *J* = 8.5 Hz, 2H), 6.81 (d, *J* = 8.6 Hz, 2H), 3.78 (s, 3H), 2.90 (dd, *J* = 13.4, 7.3 Hz, 1H), 2.80 (h, *J* = 6.9 Hz, 1H), 2.51 (dd, *J* = 13.4, 7.1 Hz, 1H), 2.41 (dq, *J* = 17.7, 7.3 Hz, 1H), 2.30 – 2.19 (m, 1H), 1.06 (d, *J* = 6.9 Hz, 3H), 0.96 (t, *J* = 7.3 Hz, 3H).

The spectral data match those reported.[16]

3-(4-methoxybenzyl)heptan-4-one (2o)

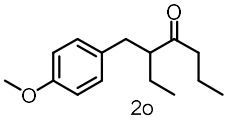

2o

Compound **2o** was synthesized following **General Procedure 3.**

A pale yellow liquid, 60% yield.

^{1}H NMR (400 MHz, CDCl3) δ 7.04 (d, *J* = 8.6 Hz, 2H), 6.80 (d, *J* = 8.6 Hz, 2H), 3.78 (s, 3H), 2.80 (dd, *J* = 13.1, 8.2 Hz, 1H), 2.71 – 2.65 (m, 1H), 2.60 (dd, *J* = 13.0, 6.1 Hz, 1H), 2.28 (dt, *J* = 17.2, 7.4 Hz, 1H), 2.12 (dt, *J* = 17.2, 7.1 Hz, 1H), 1.65 (dd, *J* = 14.1, 7.2 Hz, 1H), 1.46 (td, *J* = 7.4, 2.1 Hz, 3H), 0.84 (dt, *J* = 24.0, 7.4 Hz, 6H).

The spectral data match those reported.[17]

8. Product Standard Curve and Yield of Product

Standard Curve of **2a**:

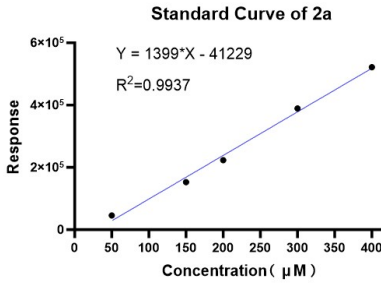

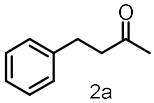

2a

Yield of the PTGR2-GDH Coupled-Enzyme Catalysis:76%
Yield of Whole-Cell Biotransformation:90%
Yield of Preparative-scale Whole-Cell Biotransformation:82%, 22.2mg

Standard Curve of **2b**:

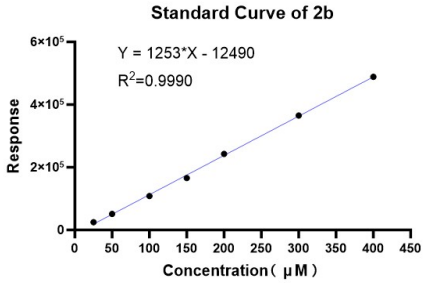

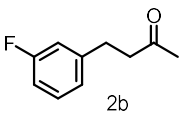

2b

Yield of the PTGR2-GDH Coupled-Enzyme Catalysis:63%
Yield of Whole-Cell Biotransformation:85%

Standard Curve of **2c**:

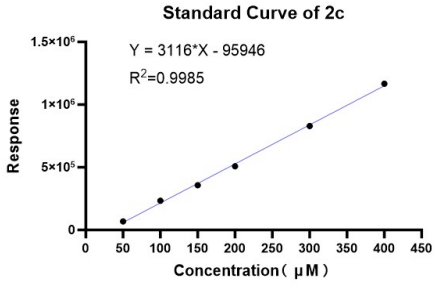

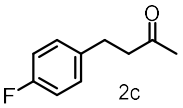

Yield of the PTGR2-GDH Coupled-Enzyme Catalysis:33%
Yield of Whole-Cell Biotransformation:83%

Standard Curve of **2d**:

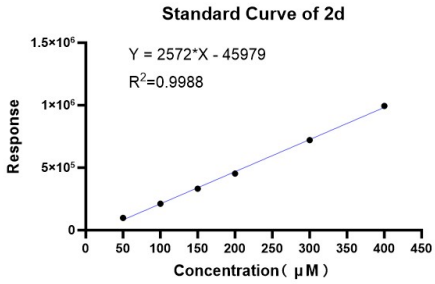

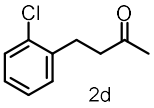

Yield of the PTGR2-GDH Coupled-Enzyme Catalysis:73%
Yield of Whole-Cell Biotransformation:72%

Standard Curve of **2e**:

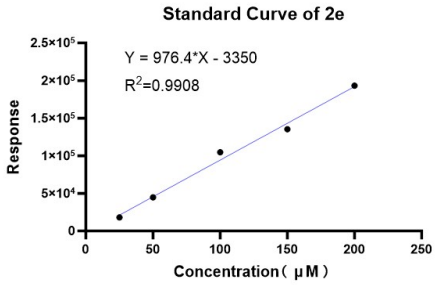

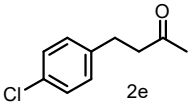

Yield of the PTGR2-GDH Coupled-Enzyme Catalysis:50%
Yield of Whole-Cell Biotransformation:78%

Standard Curve of **2f**:

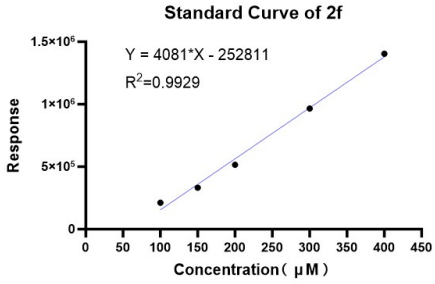

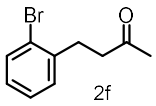

Yield of the PTGR2-GDH Coupled-Enzyme Catalysis:62%
Yield of Whole-Cell Biotransformation:70%

Standard Curve of **2g**:

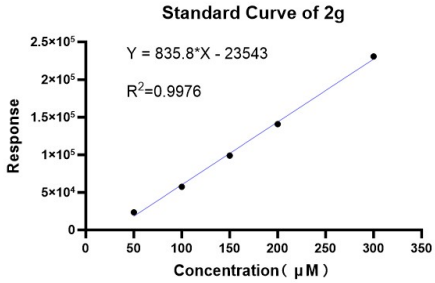

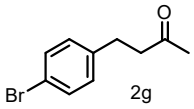

Yield of the PTGR2-GDH Coupled-Enzyme Catalysis:51%
Yield of Whole-Cell Biotransformation:69%

Standard Curve of **2h**:

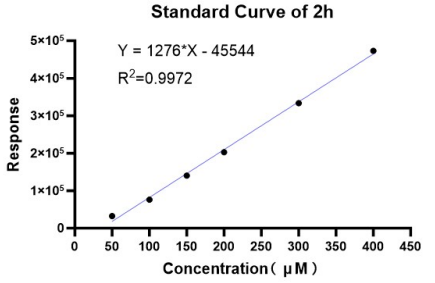

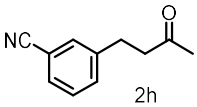

Yield of the PTGR2-GDH Coupled-Enzyme Catalysis:69%
Yield of Whole-Cell Biotransformation:83%

Standard Curve of **2i**:

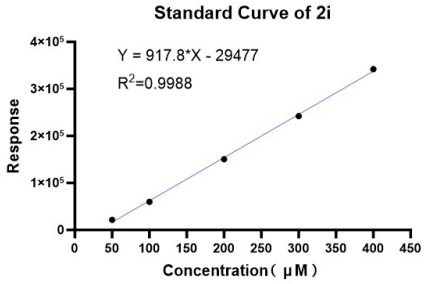

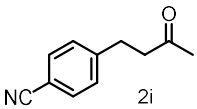

Yield of the PTGR2-GDH Coupled-Enzyme Catalysis:80%
Yield of Whole-Cell Biotransformation:88%
Yield of Preparative-scale Whole-Cell Biotransformation:81%, 26.0mg

Standard Curve of **2j**:

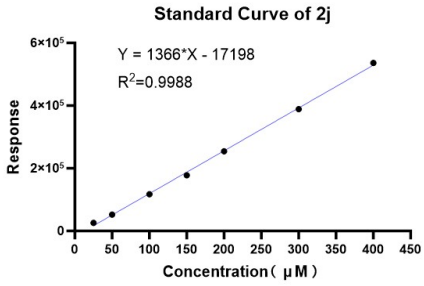

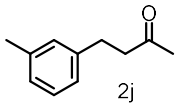

Yield of the PTGR2-GDH Coupled-Enzyme Catalysis:73%
Yield of Whole-Cell Biotransformation:73%

Standard Curve of **2k**:

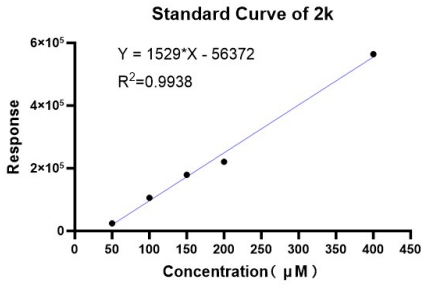

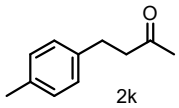

Yield of the PTGR2-GDH Coupled-Enzyme Catalysis:35%
Yield of Whole-Cell Biotransformation:81%

Standard Curve of **2l**:

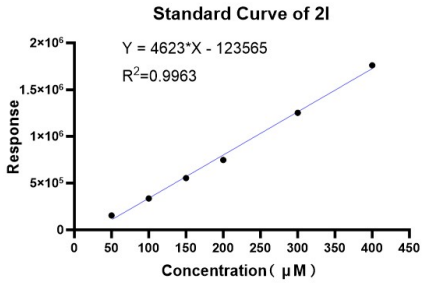

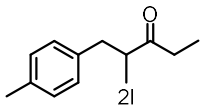

Yield of the PTGR2-GDH Coupled-Enzyme Catalysis:63%
Yield of Whole-Cell Biotransformation:85%

Standard Curve of **2m**:

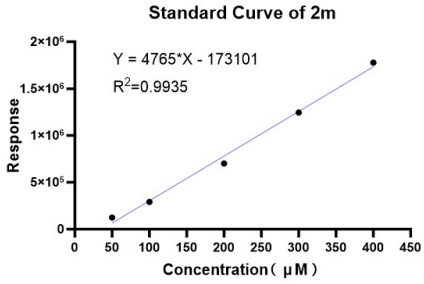

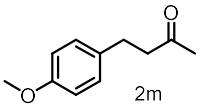

Yield of the PTGR2-GDH Coupled-Enzyme Catalysis:42%
Yield of Whole-Cell Biotransformation:90%

Standard Curve of **2n**:

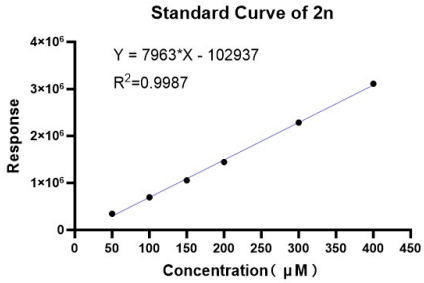

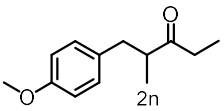

Yield of the PTGR2-GDH Coupled-Enzyme Catalysis:69%
Yield of Whole-Cell Biotransformation:83%

Standard Curve of **2o**:

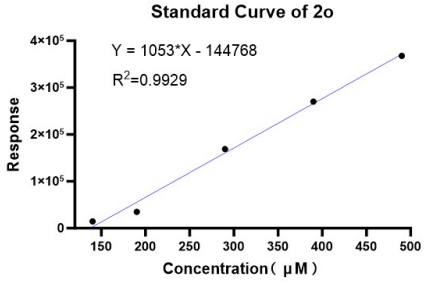

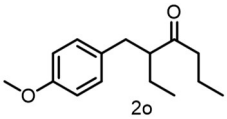

Yield of the PTGR2-GDH Coupled-Enzyme Catalysis:46%
Yield of Whole-Cell Biotransformation:84%

Standard Curve of **2p**:

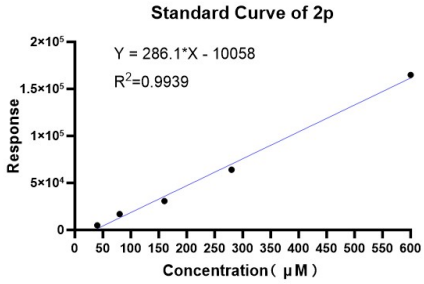

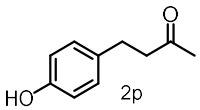

Yield of Whole-Cell Biotransformation:81%

Standard Curve of **2q**:

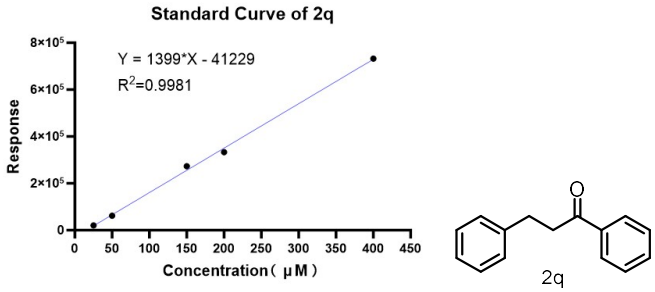

Yield of Whole-Cell Biotransformation:92%

9. NMR Spectra of Products

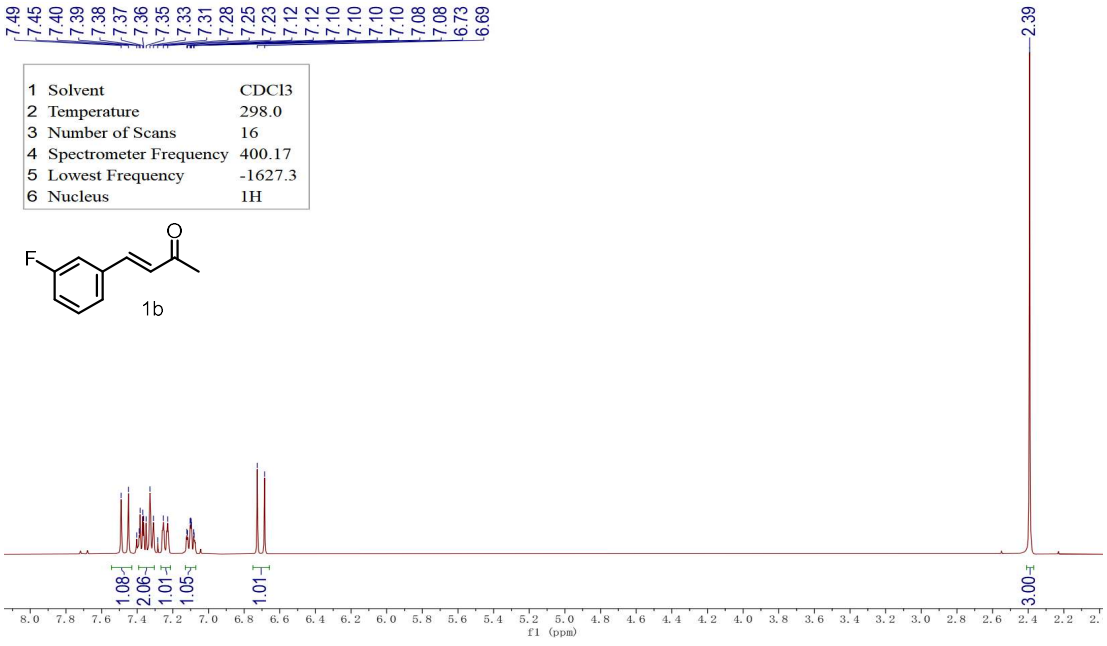

^{1}H NMR Spectrum of Compound 1b

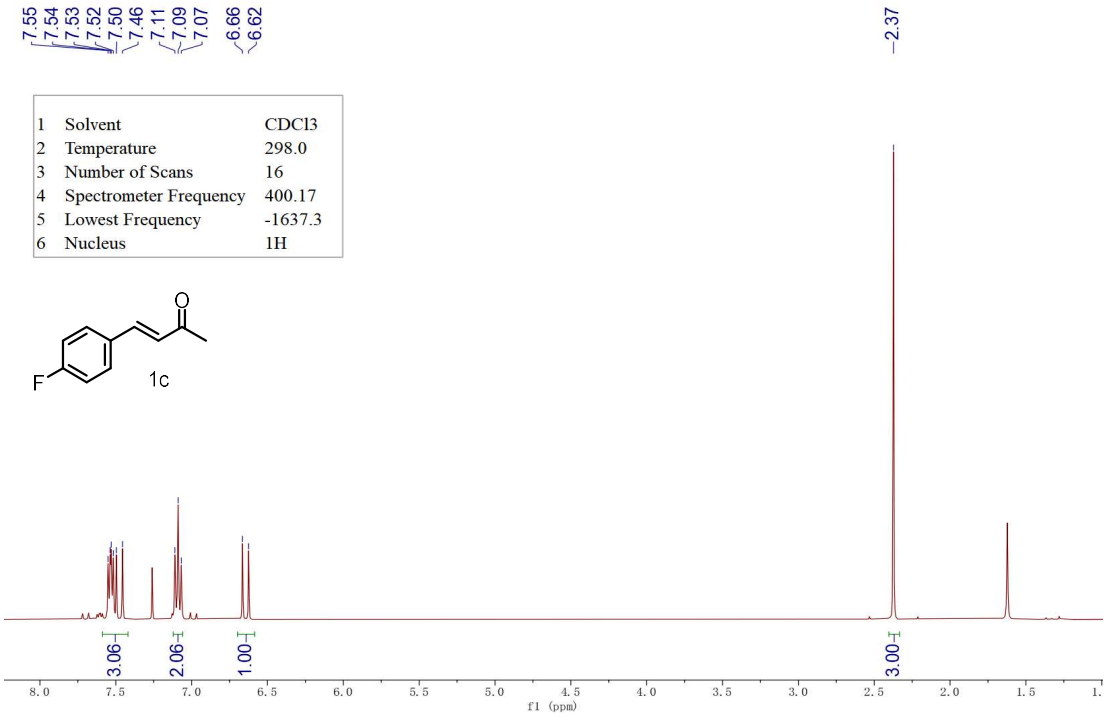

^{1}H NMR Spectrum of Compound 1c

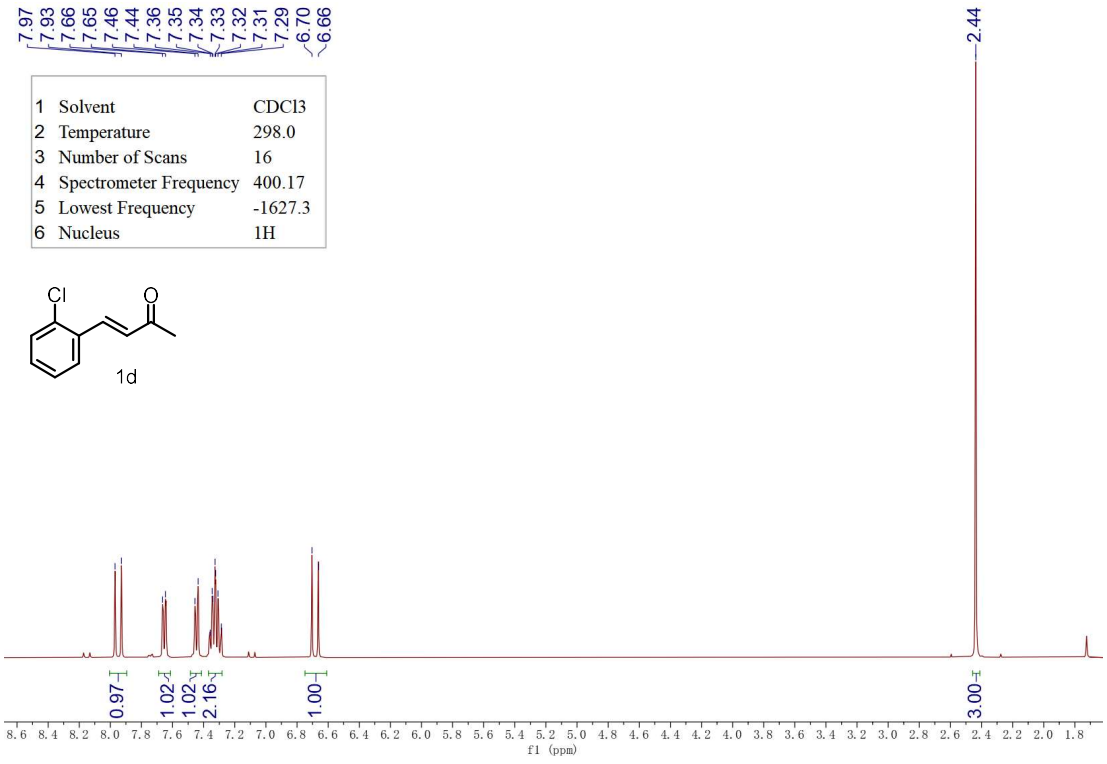

^{1}H NMR Spectrum of Compound 1d

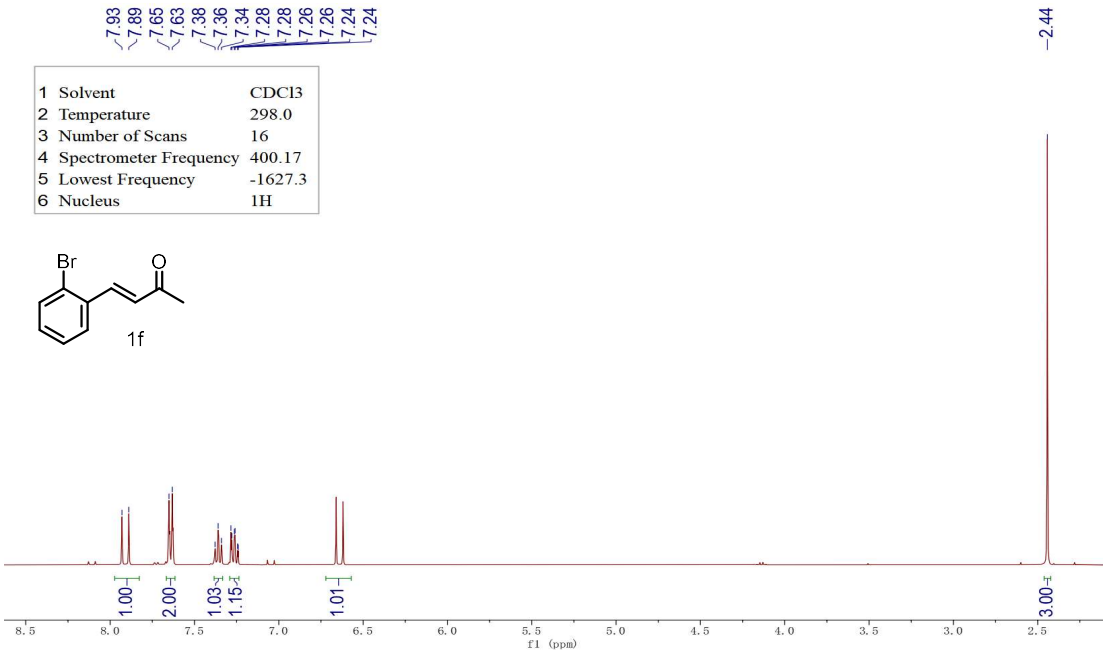

^{1}H NMR Spectrum of Compound 1f

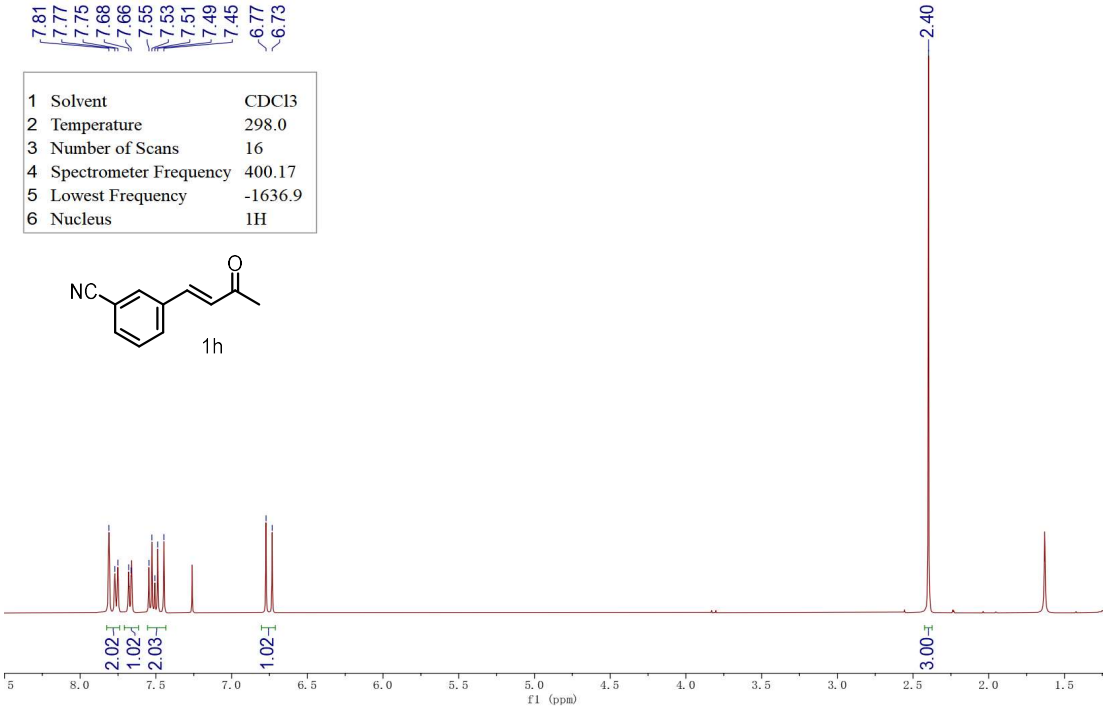

^{1}H NMR Spectrum of Compound 1h

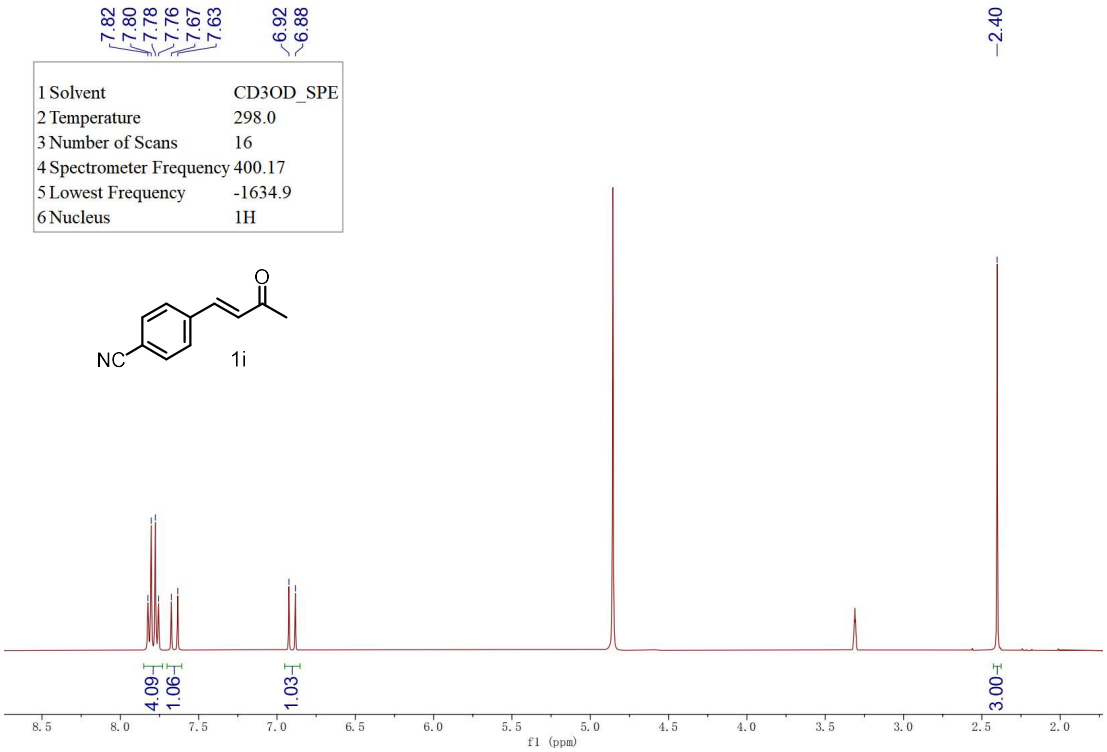

^{1}H NMR Spectrum of Compound 1i

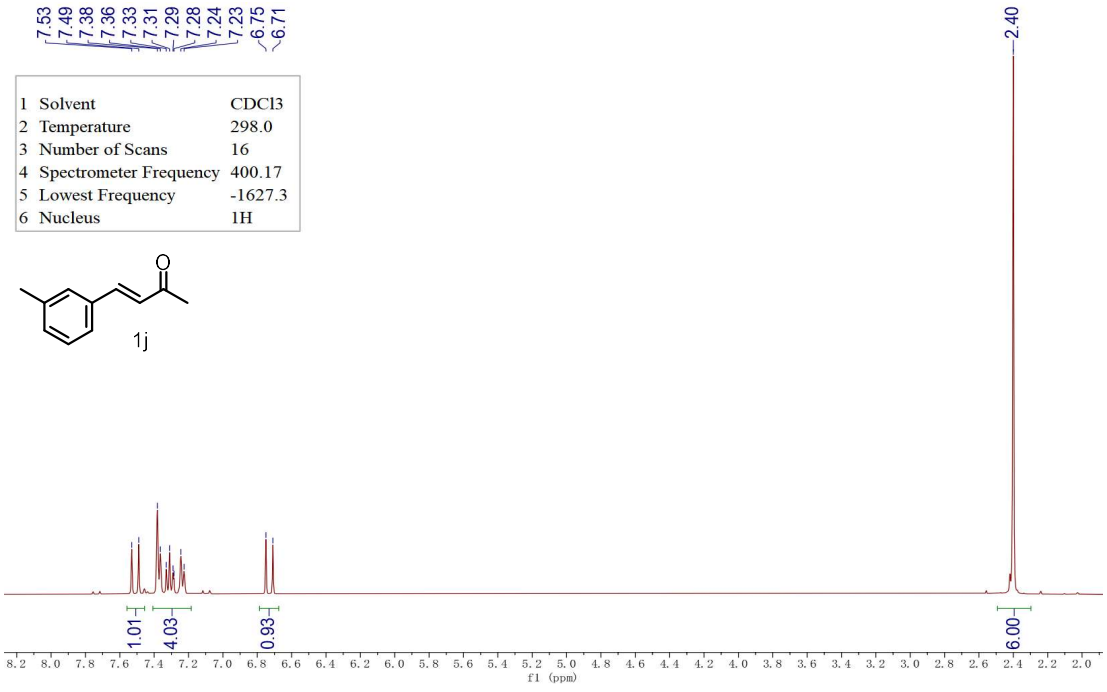

^{1}H NMR Spectrum of Compound 1j

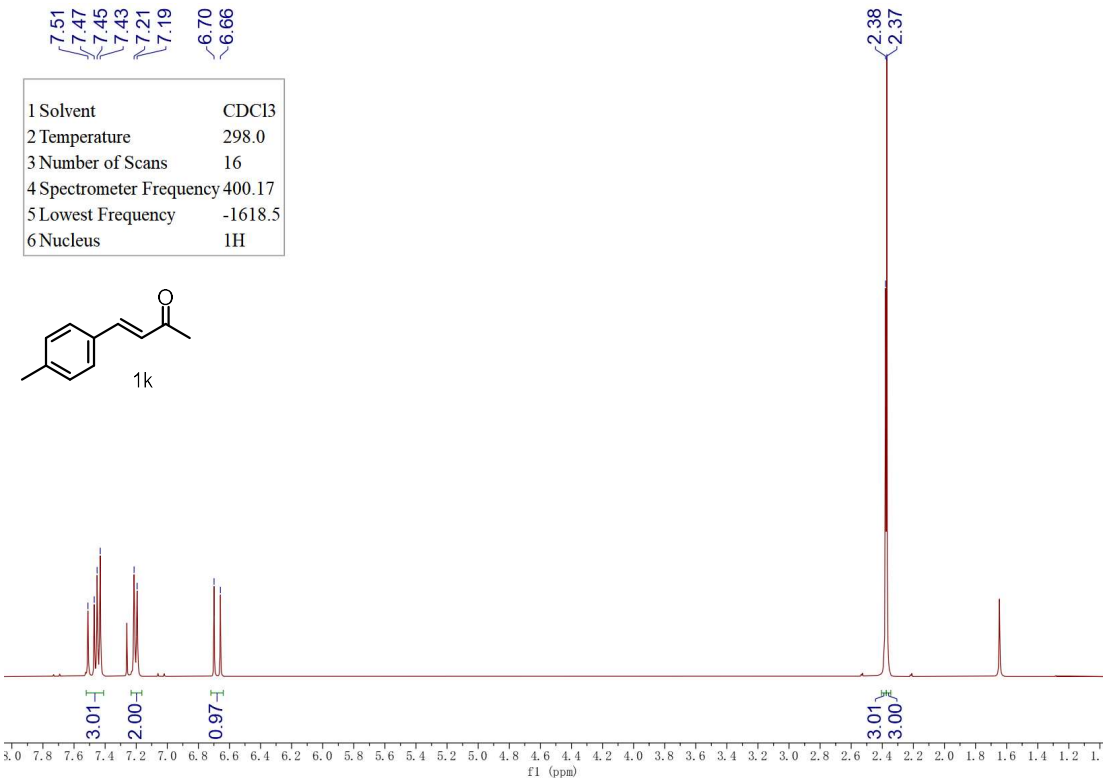

^{1}H NMR Spectrum of Compound 1k

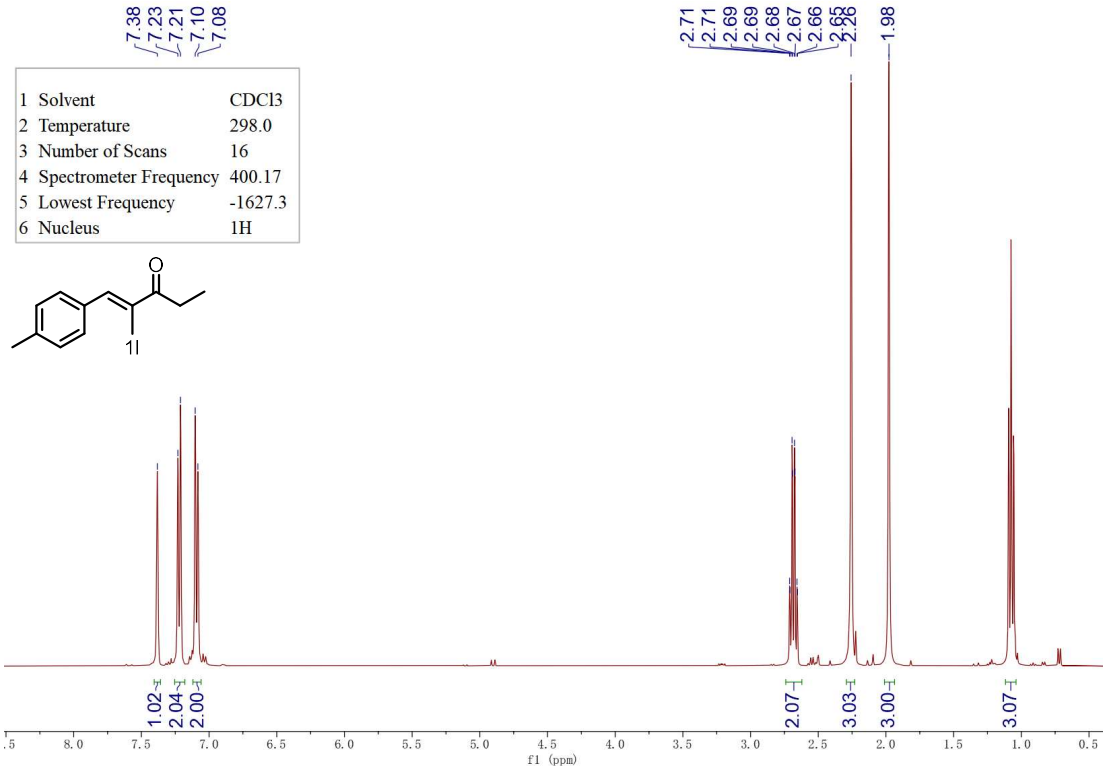

^{1}H NMR Spectrum of Compound 1l

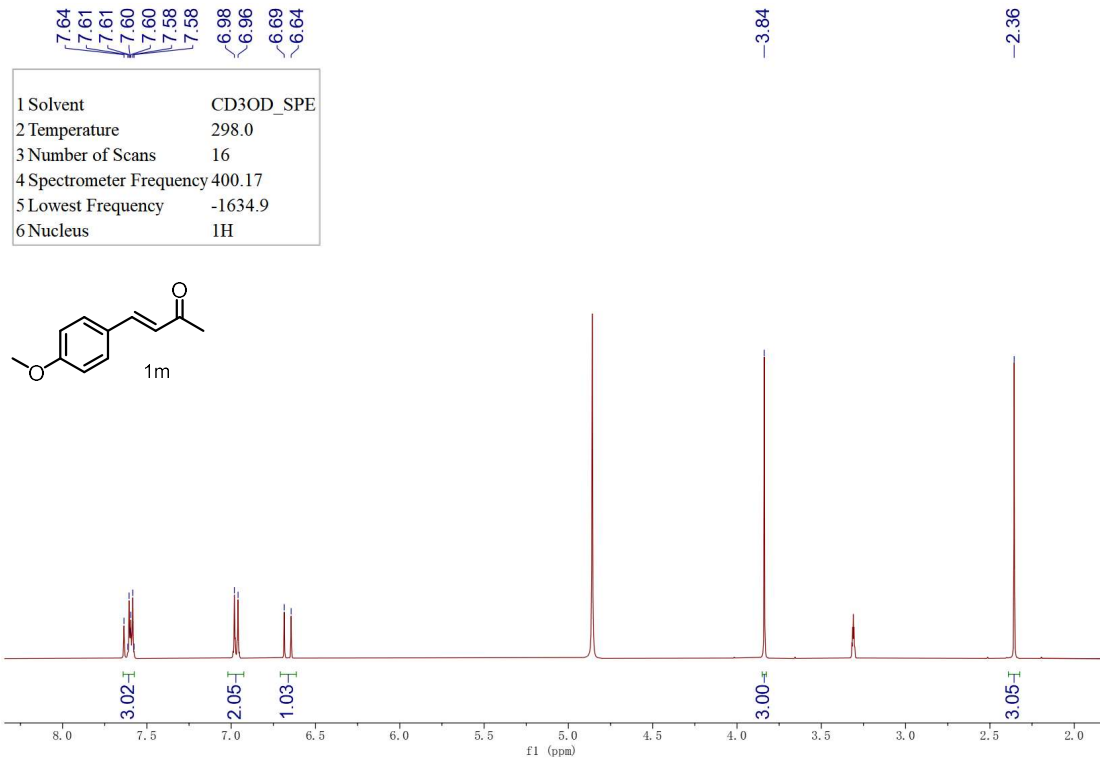

^{1}H NMR Spectrum of Compound 1m

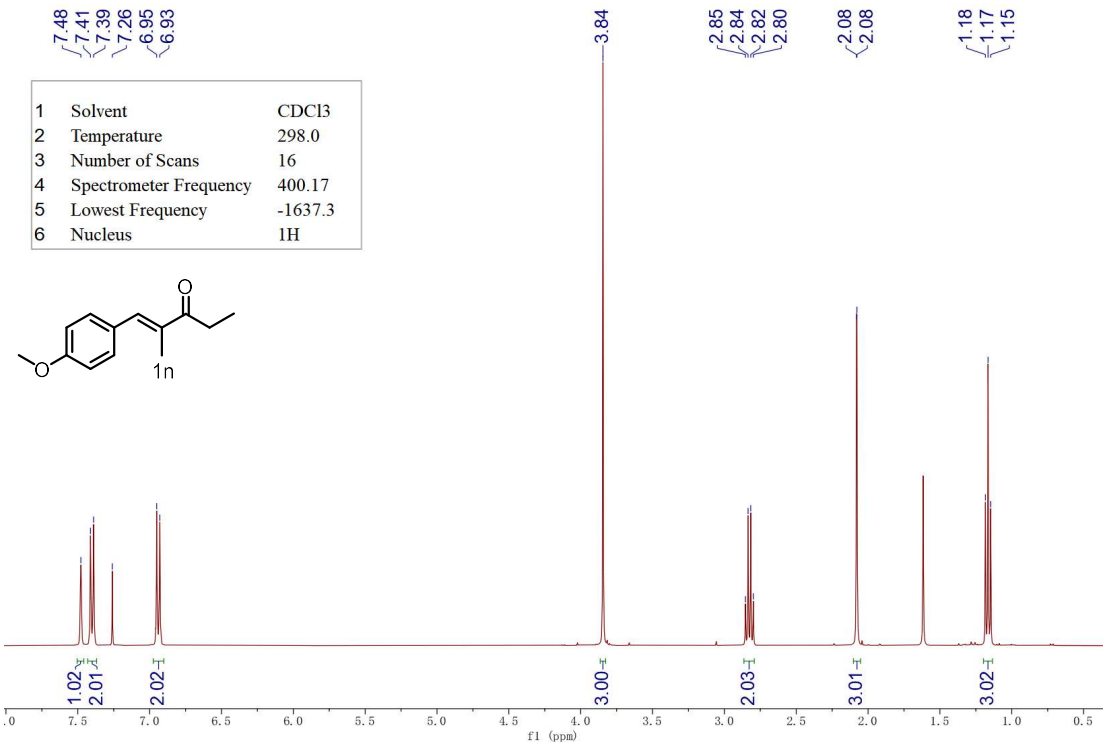

^{1}H NMR Spectrum of Compound 1n

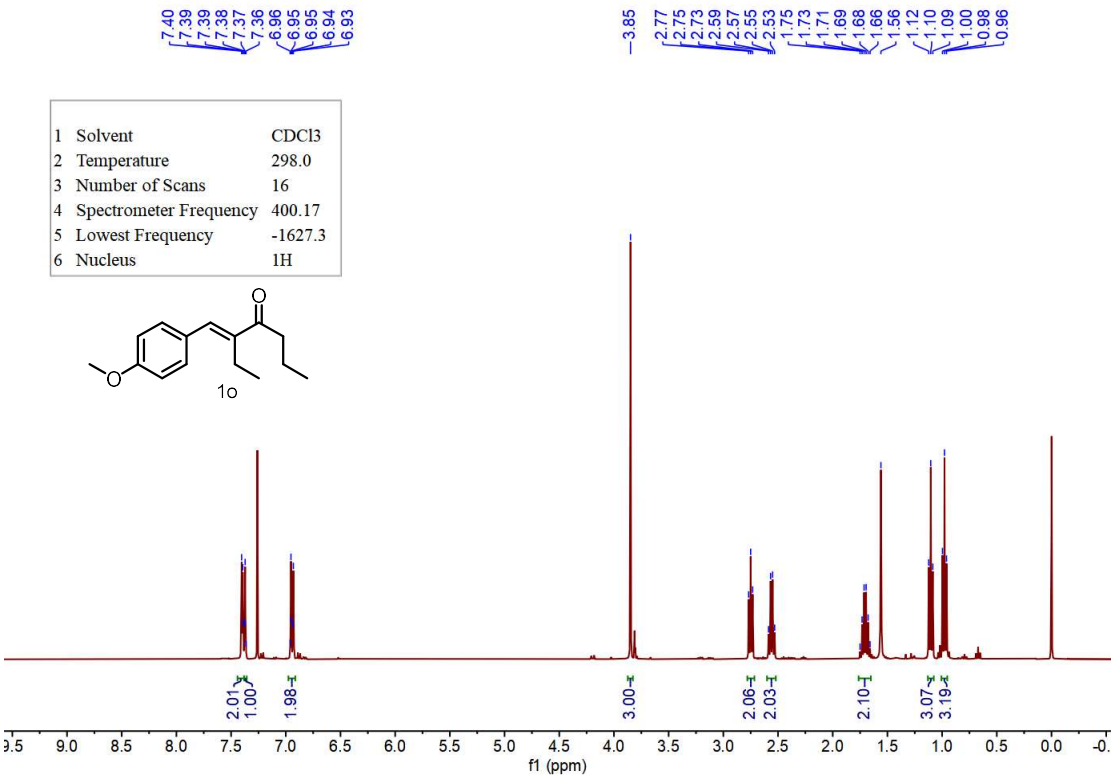

^{1}H NMR Spectrum of Compound 1o

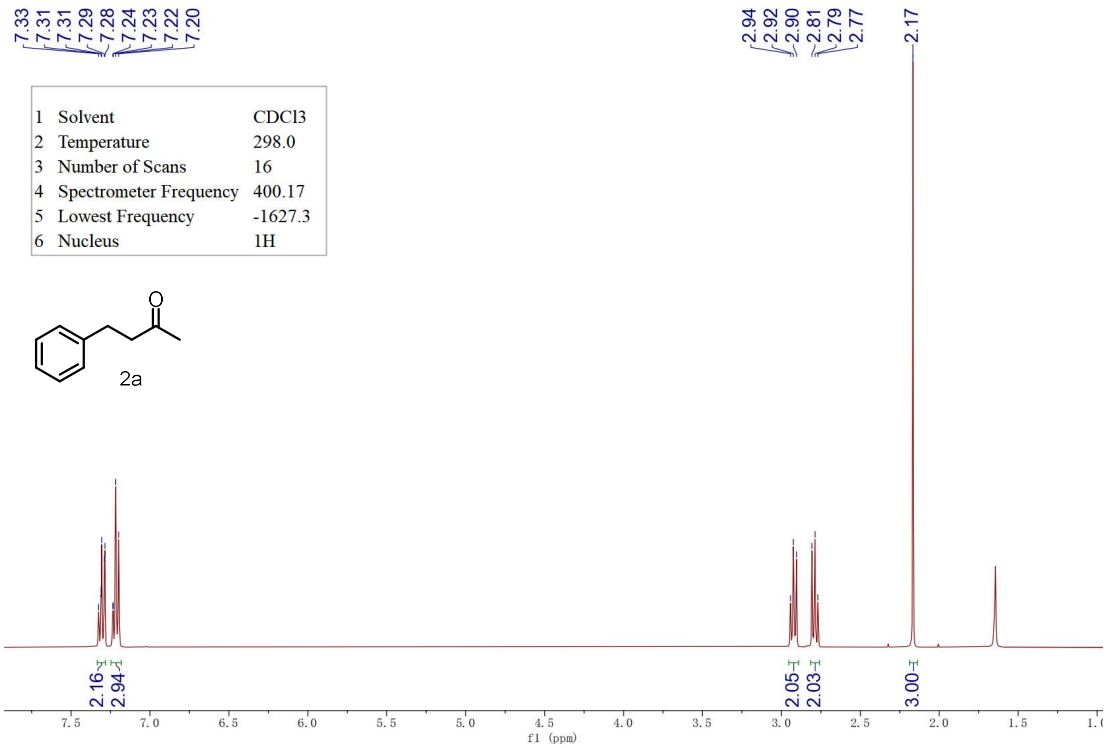

^{1}H NMR Spectrum of Compound 2a

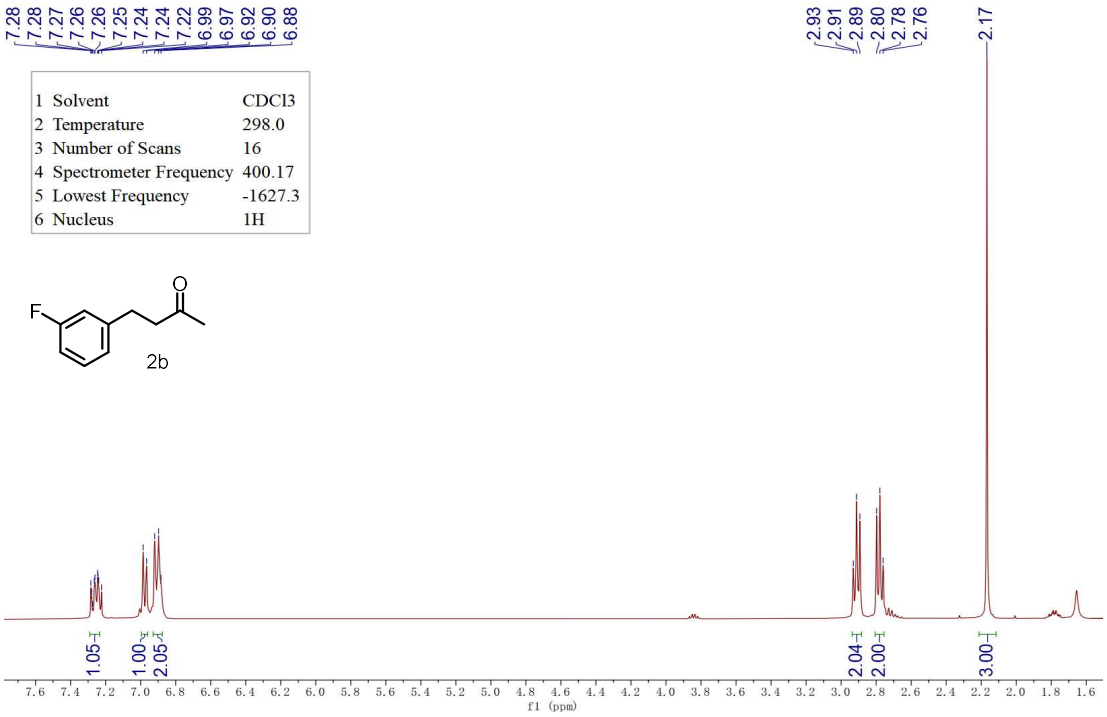

^{1}H NMR Spectrum of Compound 2b

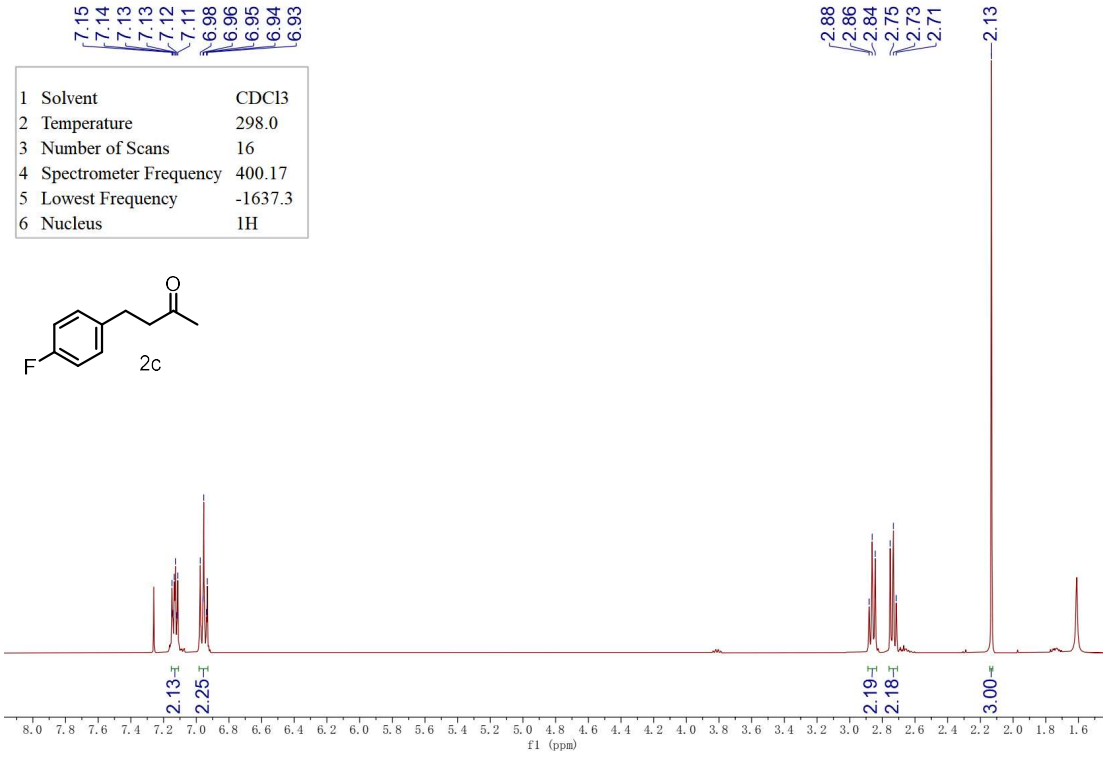

^{1}H NMR Spectrum of Compound 2c

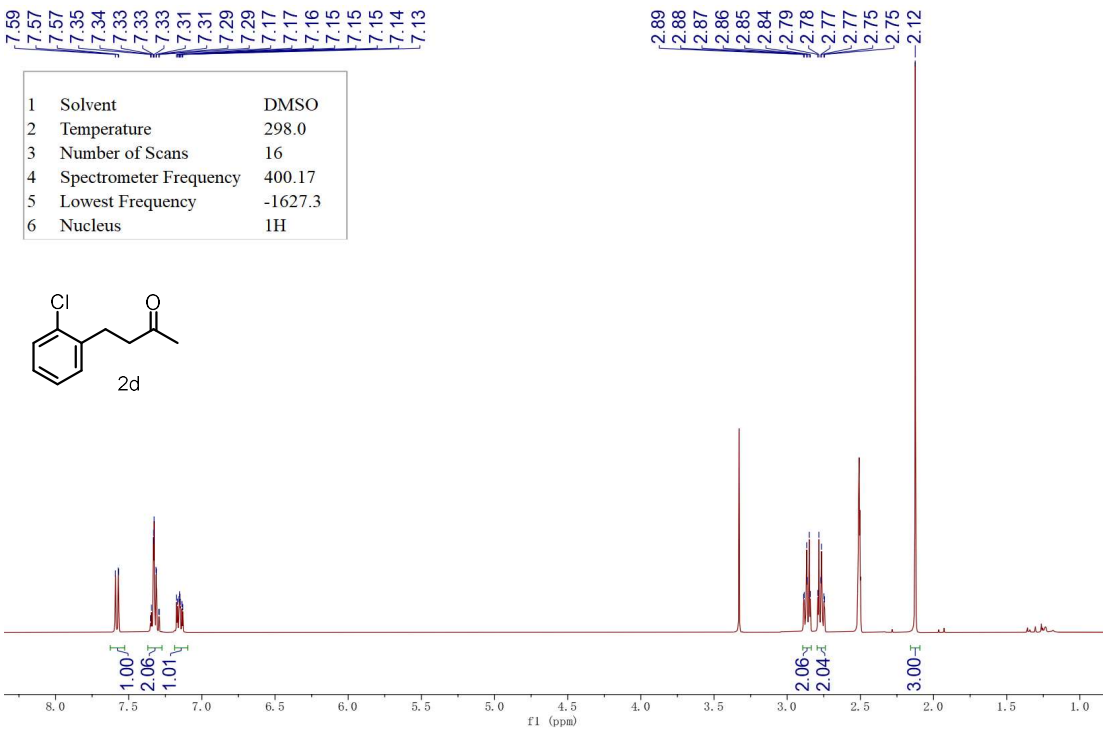

^{1}H NMR Spectrum of Compound 2d

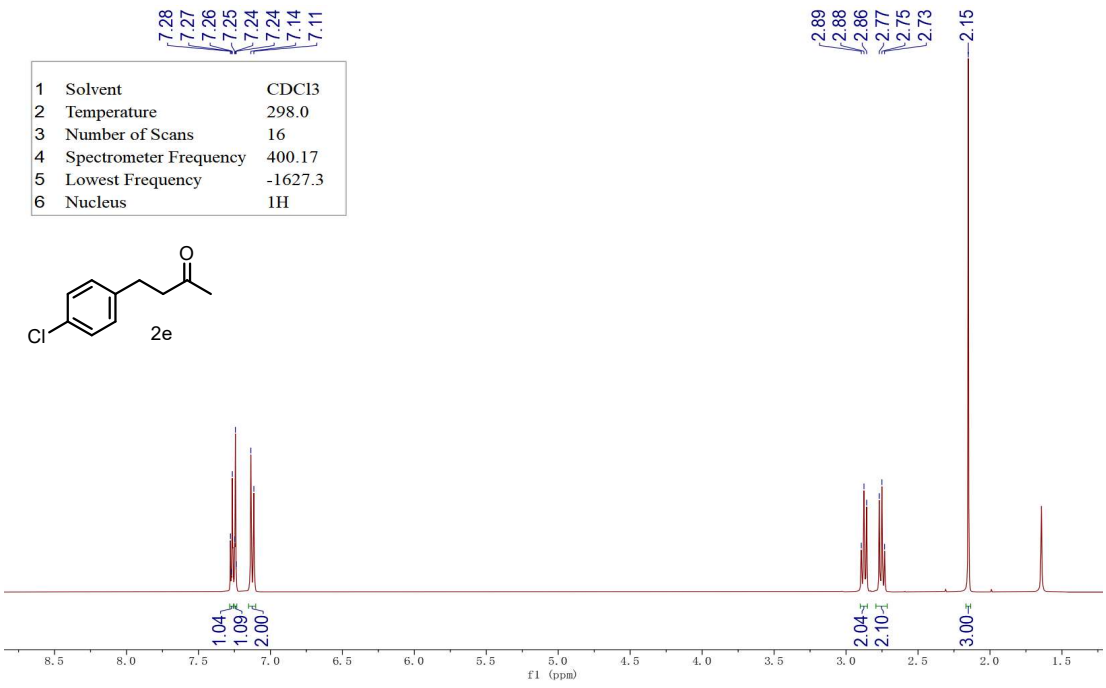

^{1}H NMR Spectrum of Compound 2e

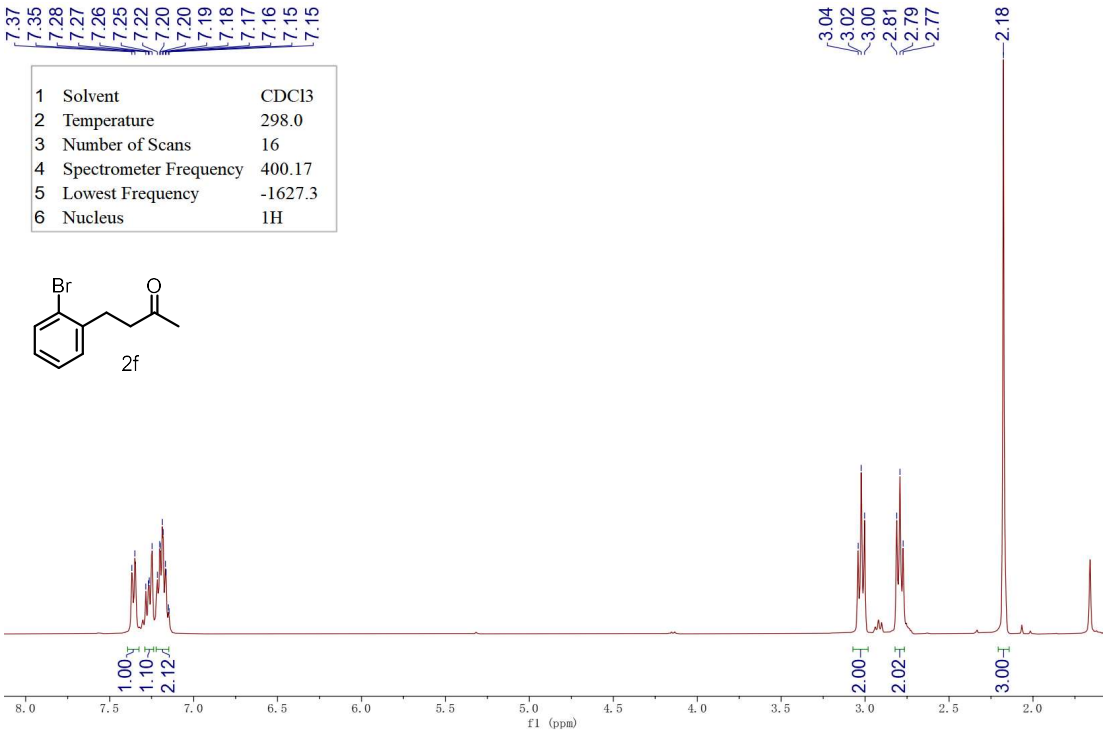

^{1}H NMR Spectrum of Compound 2f

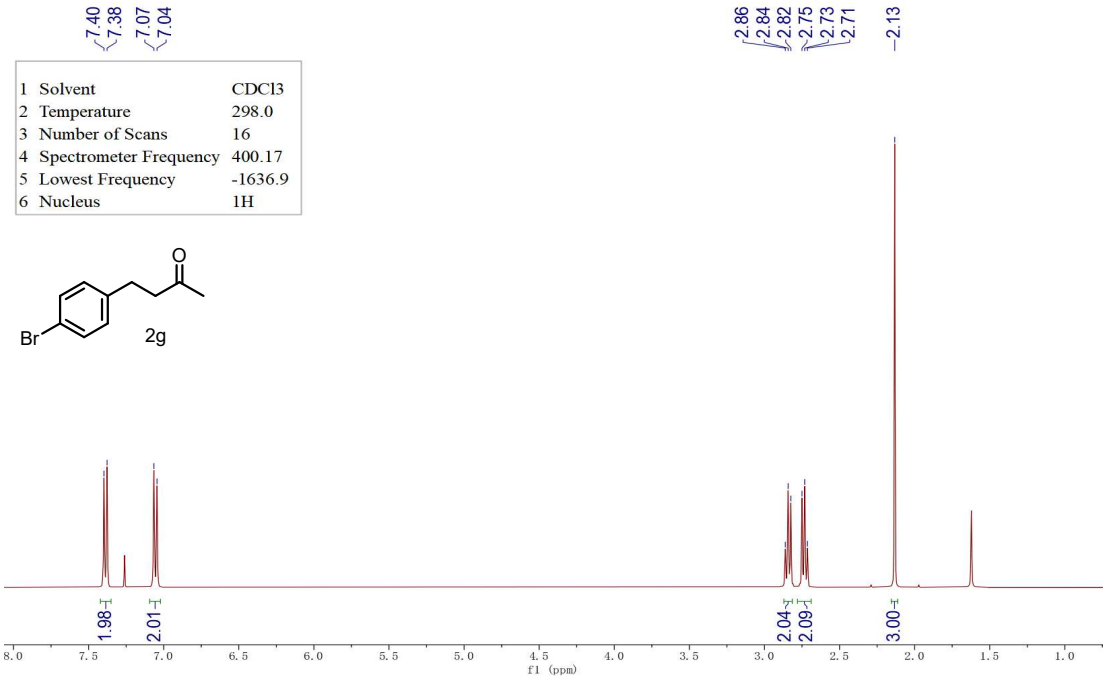

^{1}H NMR Spectrum of Compound 2g

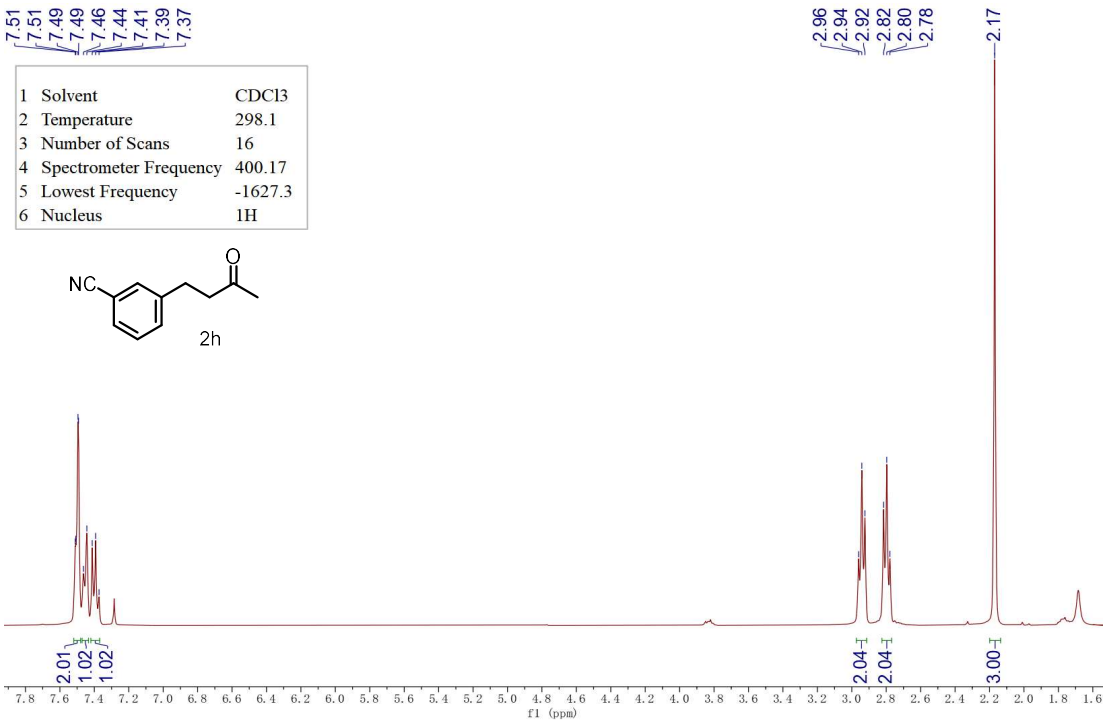

^{1}H NMR Spectrum of Compound 2h

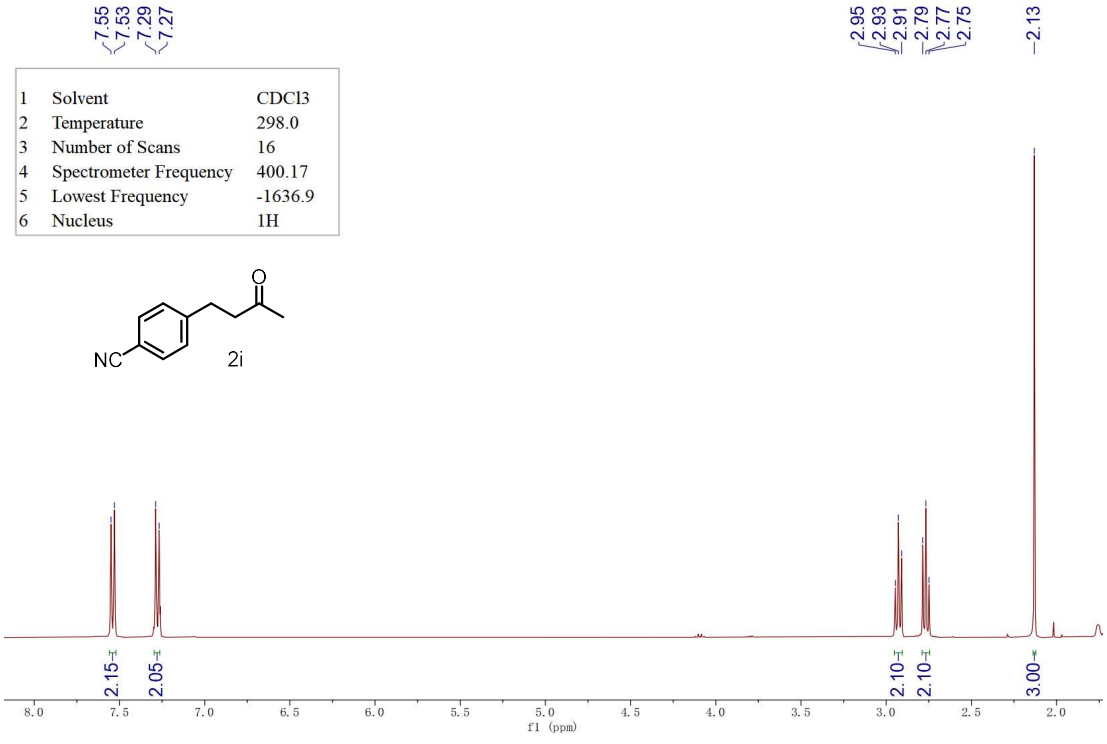

^{1}H NMR Spectrum of Compound 2i

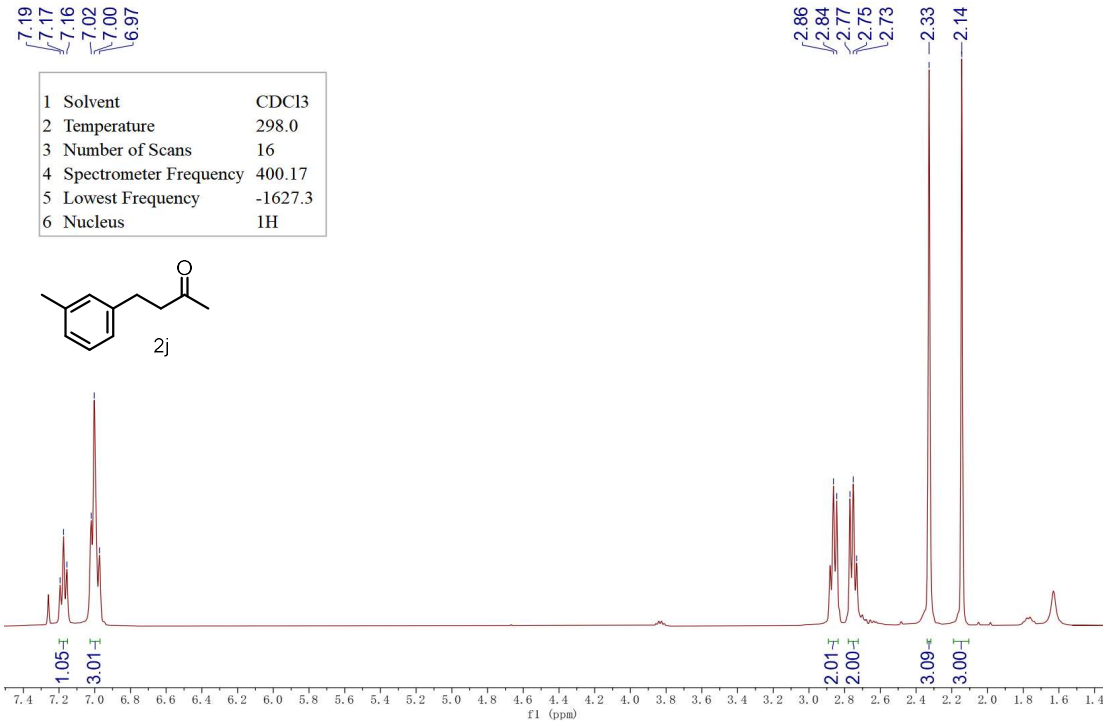

^{1}H NMR Spectrum of Compound 2j

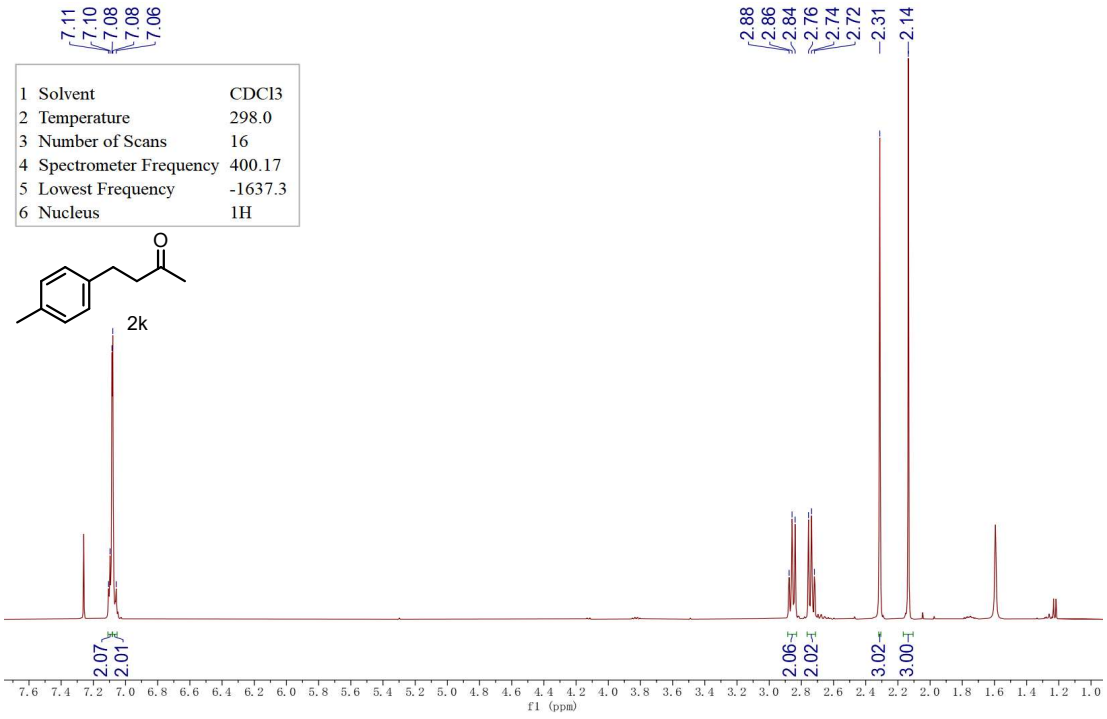

^{1}H NMR Spectrum of Compound 2k

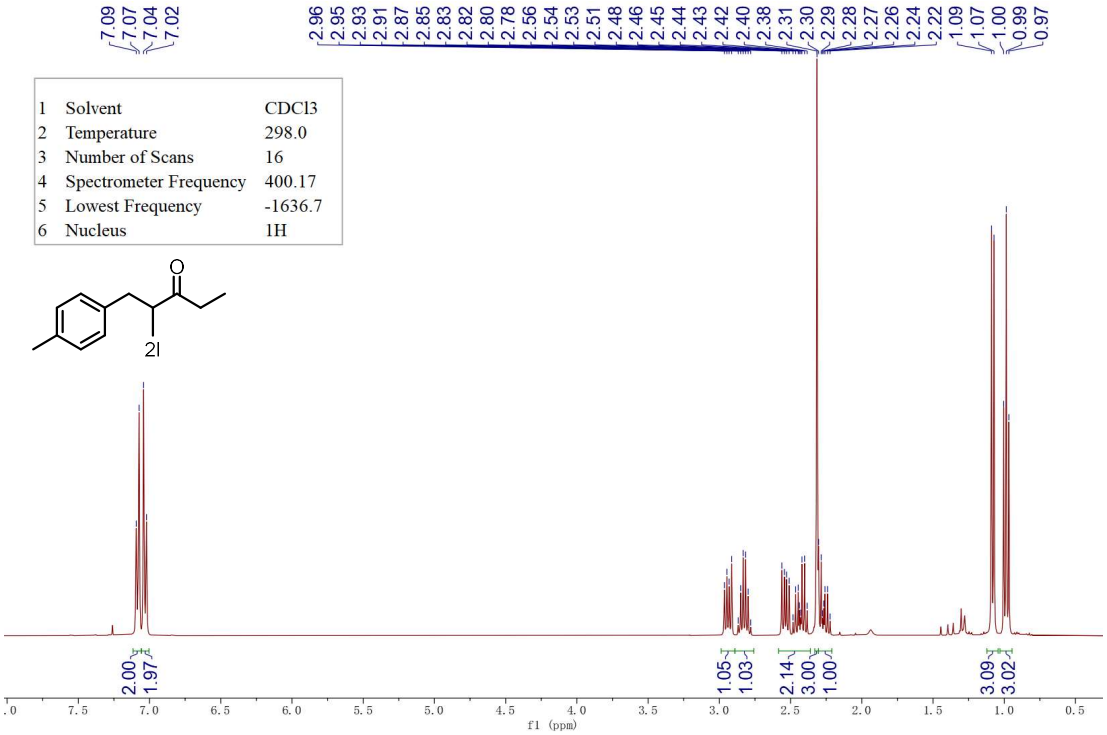

^{1}H NMR Spectrum of Compound 2l

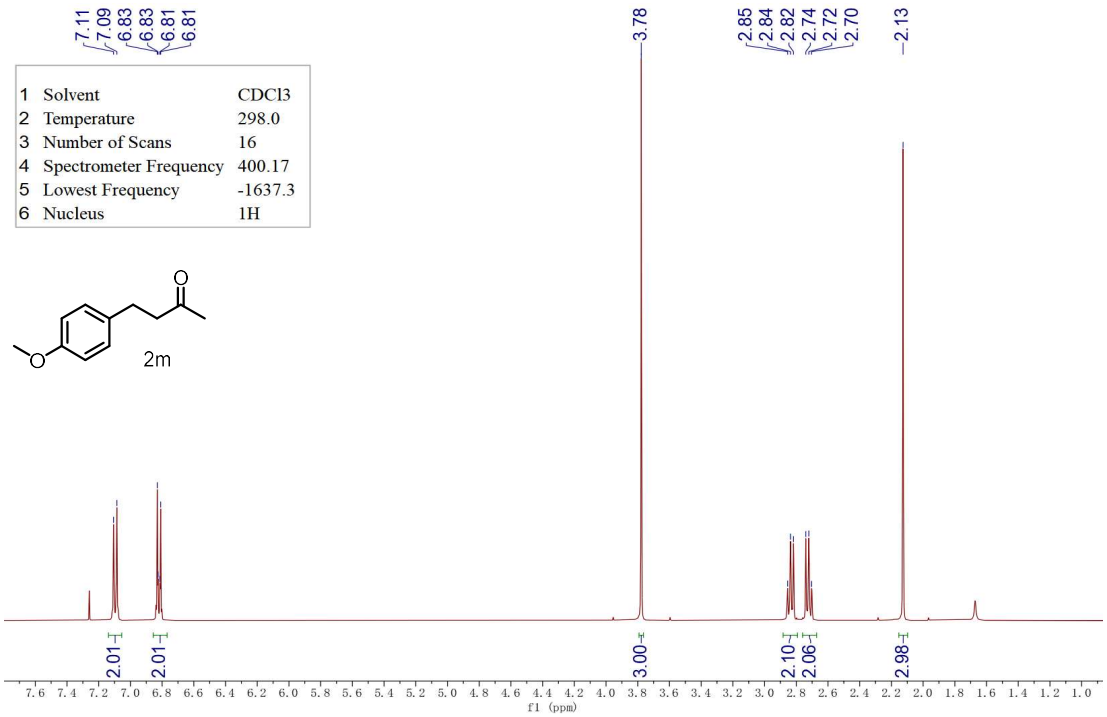

^{1}H NMR Spectrum of Compound 2m

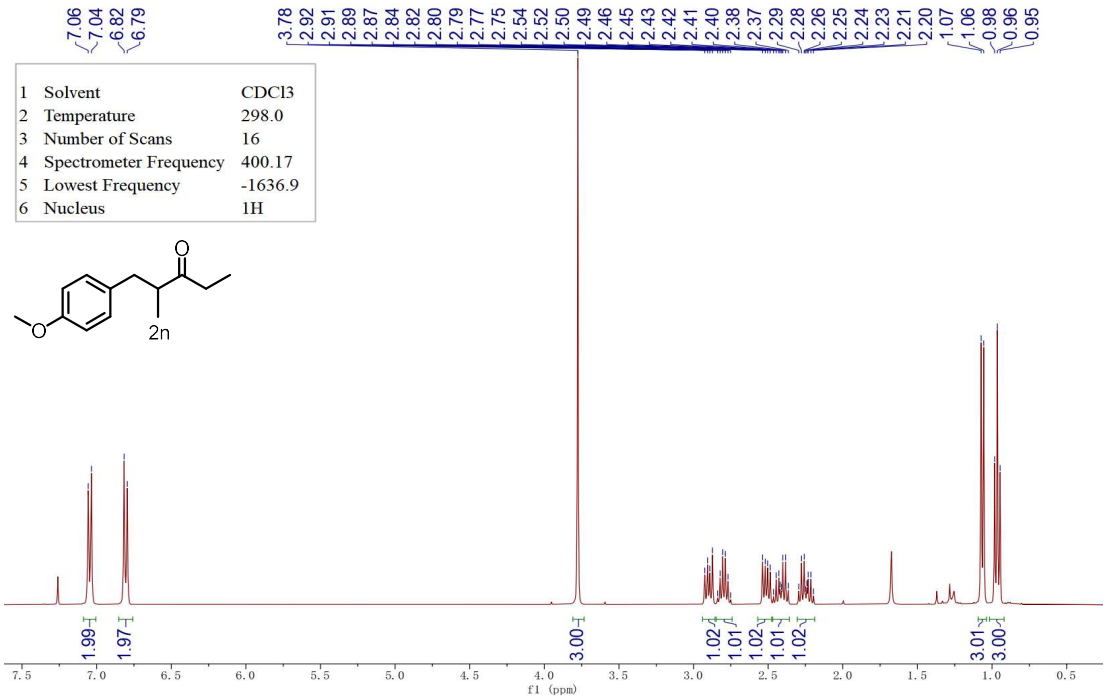

^{1}H NMR Spectrum of Compound 2n

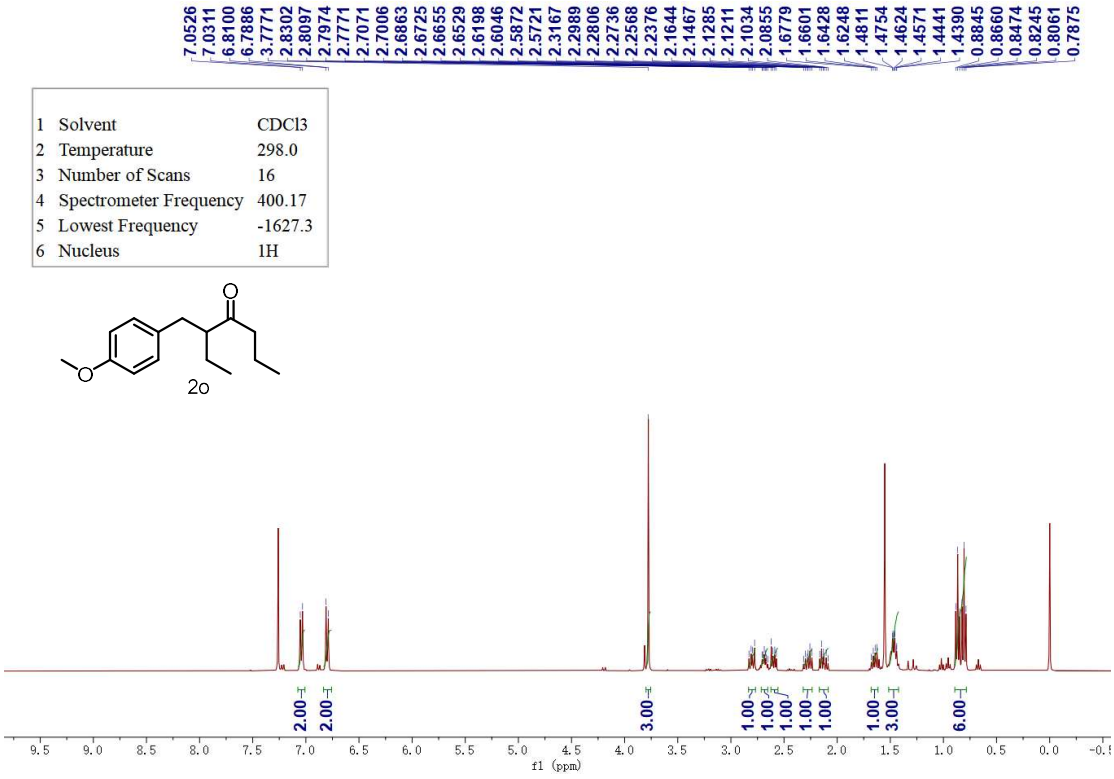

^{1}H NMR Spectrum of Compound 2o

10. References

1. Trott O and Olson AJ. AutoDock Vina: improving the speed and accuracy of docking with a new scoring function, efficient optimization, and multithreading. *J Comput Chem* 2010; 31: 455-461. 2009/06/06. DOI: 10.1002/jcc.21334.
2. Viji M, Jothi SS, Yasiha K, et al. Molecular docking analysis of Naringenin from the leaves of Psidium guajava as a promising agent for breast cancer therapy. *Journal of Medico Informatics* 2025; 1: 35-43. DOI: 10.64659/jomi/210351.
3. Wu Y-H, Ko T-P, Guo R-T, et al. Structural Basis for Catalytic and Inhibitory Mechanisms of Human Prostaglandin Reductase PTGR2. *Structure* 2008; 16: 1714-1723. DOI: 10.1016/j.str.2008.09.007.
4. Liu YW, Li LJ, Xu H, et al. Palladium-Catalyzed Alkynylation of Enones with Alkynylsilanes via C-C Bond Activation. *J Org Chem* 2022; 87: 6807-6811. 2022/05/05. DOI: 10.1021/acs.joc.2c00498.
5. Lu SM and Bolm C. Highly enantioselective synthesis of optically active ketones by iridium-catalyzed asymmetric hydrogenation. *Angew Chem Int Ed Engl* 2008; 47: 8920-8923. 2008/10/16. DOI: 10.1002/anie.200803709.
6. Choi H, Ham SY, Cha E, et al. Structure-Activity Relationships of 6- and 8-Gingerol Analogs as Anti-Biofilm Agents. *J Med Chem* 2017; 60: 9821-9837. 2017/11/15. DOI: 10.1021/acs.jmedchem.7b01426.
7. Wang Y, Du ZH, Bo C, et al. Synthesis of alpha,beta-Unsaturated Carbonyl Compounds via Cu/TEMPO/O(2) Aerobic Catalytic System. *Chemistry* 2025; 31: e202403950. 2025/01/09. DOI: 10.1002/chem.202403950.
8. Zhu D, Cao Y, Qian Y, et al. Preparation of Amino-Modified Ti3C2/Mg3Al-LDH Composites and Their Application in Aldol Reaction. *ChemCatChem* 2025; 17. DOI: 10.1002/cctc.202401809.
9. Zeng B-B, Chen W-D, Liu J, et al. Copper-Catalyzed One-Pot Oxidation–Aldol/Henry Reaction of Benzylic -Amines to α,β-Unsaturated Methyl Ketone/Nitro Compounds. *Synlett* 2013; 24: 2740-2742. DOI: 10.1055/s-0033-1338986.
10. Syamala LVRB, Khopade TM, Warghude PK, et al. An access to α, β-unsaturated ketones via dual cooperative catalysis. *Tetrahedron Letters* 2019; 60: 88-91. DOI: 10.1016/j.tetlet.2018.11.065.
11. Woo JCS, Walker SD and Faul MM. Preparation and decarboxylative rearrangement of (Z)-enyne esters. *Tetrahedron Letters* 2007; 48: 5679-5682. DOI: 10.1016/j.tetlet.2007.06.012.
12. Xi J, Ng EWH and Ho C-Y. Unsymmetric N-Aryl Substituent Effects on Chiral NHC-Cu: Enantioselectivity and Reactivity Enhancement by Ortho-H and Syn-Configuration. *ACS Catalysis* 2022; 13: 407-421. DOI: 10.1021/acscatal.2c03942.
13. Dong XY, Lin Y, Cui YM, et al. PMHS-Containing Semi-Penetrating Networks as Multifunctional Hydrosilanes for Highly Efficient Palladium-Catalyzed Conjugate Reduction of Enones. *ChemistrySelect* 2016; 1: 2400-2404. DOI: 10.1002/slct.201600667.

14. Jiang C, Wu Y, Zhang Y, et al. Supramolecular Modulation for Selective Mechanochemical Iron-Catalyzed Olefin Oxidation. *Angew Chem Int Ed Engl* 2025; 64: e202413901. 2024/09/02. DOI: 10.1002/anie.202413901.
15. Condon S, Dupré D, Falgayrac G, et al. Nickel-Catalyzed Electrochemical Arylation of Activated Olefins. *European Journal of Organic Chemistry* 2002; 2002: 105-111. DOI: 10.1002/1099-0690(20021)2002:1<105::Aid-ejoc105>3.0.Co;2-j.
16. Onishi Y, Nishimoto Y, Yasuda M, et al. InCl3/Me3SiBr-catalyzed direct coupling between silyl ethers and enol acetates. *Org Lett* 2011; 13: 2762-2765. 2011/04/30. DOI: 10.1021/ol200875m.
17. Zhang L, Yang G, Shen C, et al. Chiral dinuclear phthalazine bridged bisoxazoline ligands: synthesis and application in enantioselective Cu-catalyzed conjugate addition of ZnEt2 to enones. *Tetrahedron Letters* 2011; 52: 2375-2378. DOI: 10.1016/j.tetlet.2011.02.098.